Chapter 7

TARGET PARAMETER ESTIMATION

W. K. Hocking [1]

Radio Atmospheric Science Center,
Kyoto University, Uji, Kyoto 611, JAPAN

Abstract

The objective of any radar experiment is to determine as much about the entities which scatter the radiation as possible. This review discusses many of the various parameters which can be deduced in a radar experiment, and also critically examines the procedures used to deduce them. Methods for determining the mean wind velocity, the RMS fluctuating velocities, turbulence parameters (e.g. C_n^2, ϵ, K_M), and the shapes of the scatterers are considered. Complications with these determinations are discussed. It is seen throughout that a detailed understanding about the shape and cause of of the scatterers is important in order to make better determinations of these various quantities. Finally, some other parameters, which are less easily acquired, are considered. For example, it is noted that momentum fluxes due to buoyancy waves and turbulence can be determined, and on occasions radars can be used to determine stratospheric diffusion coefficients and even temperature profiles in the atmosphere.

1 Introduction

The ultimate aim of any radar experiment is of course to determine information about the structures which backscatter the radio waves, and the environment in which they exist. For example, it might be of interest to study the shape of the scatterers, or to differentiate different types of scatterers or reflectors. It might be of interest to determine the radar cross-section of the scatterers, or their spatial distribution over the sky. Other desired information might include the velocity of the scatterers, and information about the spatial and temporal variation of these velocities. If the radio scatter is due to the turbulence, it might be desirable to measure the intensity of the turbulence.

The purpose of this article is to discuss ways in which parameters like these can be determined, and how they can be interpreted. Some of the approximations used in determining these parameters are also critically examined. Some consideration will be given to experimental design, and then interpretation of the results. Studies of the parameters evaluated over long periods of time can give a considerable amount of additional information, over and above that which can be determined from a few discrete observations, but discussion of this aspect will not be considered in great detail, due to lack of space.

The paper is organized in such a way that the simplest parameters are discussed first, and parameters which are more difficult to extract are considered later.

2 Wind vector determination

One of the the simplest and yet most important parameters to determine is the wind speed, so we shall begin with a brief discussion of its determination, examining in detail some of the

[1] On leave from Department of Physics and Mathematical Physics,
University of Adelaide, S.A., 5001 Australia

assumptions made in this evaluation.

There are at least two different approaches to the determination of the mean wind. One utilizes large antenna arrays with correspondingly narrow radiation patterns, and with the beams pointed in various directions to measure wind speeds; the Doppler shift of the backscattered signal is utilized for this calculation, and such techniques are called "Doppler Beam Swinging" (DBS) techniques. The second class of method, called spaced antenna methods, utilizes systems of separated (spaced) arrays; wind speeds are determined by using phase and time differences between signals received with the arrays. The sets of spaced antenna arrays usually have smaller physical dimensions than the antenna arrays used in the DBS mode. In some senses, the techniques which use time delays and the techniques which utilize phase delays can even be regarded as distinct techniques, and they will be considered somewhat independently in this paper; however they will both be considered as "spaced antenna" techniques. These various different approaches will now be discussed.

2.1 Doppler measurements

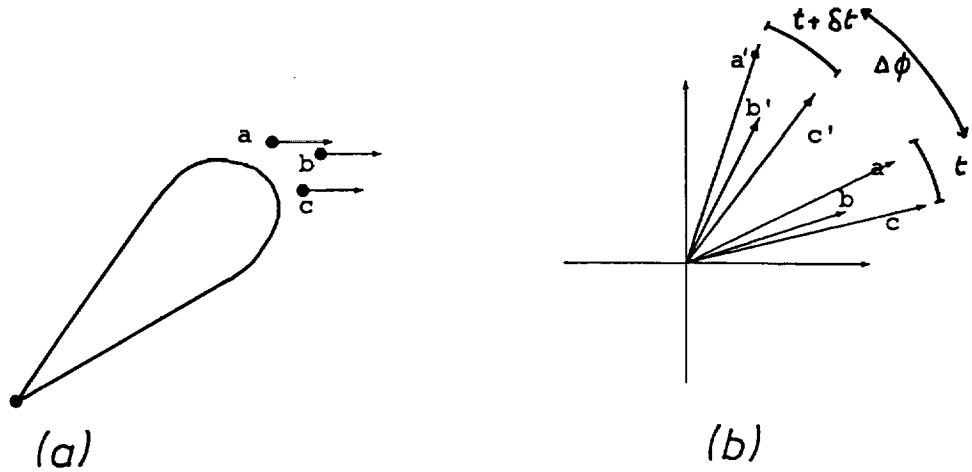

Fig. 1 Principle of Doppler method; off-vertical beam used to record rate of change of phase of scatterers.

The principle of Doppler determination of the wind speed is to utilize the change in the phase of scattered radio waves as a function of time. It is probably the most common procedure currently in use, so some time will be devoted to discussion of this technique.

2.1.1 Basic principles of the Doppler method

As the scatterers move, the path length between the transmitter, scatterer and receiver changes, and this shows as a change in phase (fig. 1a). We can think of this as the rotation of the vector in the argand plane (fig. 1b). For a monostatic radar, the mean rate of change of phase is a measure of the mean radial component of the velocity of the scatterers viz.

$$< v_{rad} >= \frac{\lambda}{4\pi} < \frac{d\phi}{dt} > \qquad (1)$$

Here, <> represents the average value, averaged over the radar volume and the sampling time, v_{rad} is the radial component of the velocity, λ is the radar wavelength, ϕ is the phase, and $d\phi/dt$ is the rate of change of phase. Each scatterer causes its appropriate vector to rotate at a slightly different frequency, and we can represent this on a spectrum, where each line corresponds to a different scatterer (fig. 2). Of course it should be borne in mind that in a real spectrum, it may not be physical to think of each separate spectral line as due to such a scatterer, but for our purposes this is adequate.

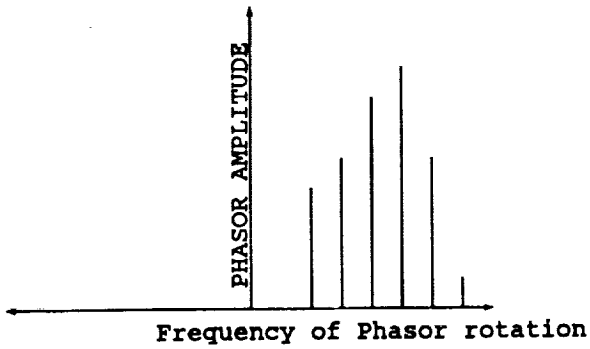

Fig. 2

We shall assume for simplicity that the spectral density and frequency of each line is invariant, so just the phase of the signal from each scatterer changes. If a single phasor at time t can be described by $\underline{a}_0 = a_0 e^{i\omega t}$, ($a_0 = \mid \underline{a}_0 \mid$) then at time $t + \delta t$ it is given by $\underline{a}_0' = a_0 e^{i\omega(t+\delta t)}$. Given the two phasors, the phase difference can be found by calculating $\underline{a}_0^* \cdot \underline{a}_0'$, where (*) means complex conjugate. This calculation gives $a_0^2 e^{i\omega\delta t} = a_0^2 e^{i\Delta\phi}$. We actually seek $< \Delta\phi >$ averaged over all the scatterers in the radar volume, but if the phasors all have equal amplitude, or even more generally the spectrum has a symmetric shape, then we can say that $< \Delta\phi >= arg\{< a^2 e^{i\Delta\phi} >\}$, even for large values of $\Delta\phi$. In other words, summing the phasors and finding the rotation of the resultant gives the same result as averaging the angles of rotation of each phasor. This is also true even in the presence of a moderate amount of noise. Hence we will consider averages of $a_0^2 e^{i\Delta\phi}$. This mean value calculated for n phasors $a_j e^{i\Delta\phi_j}$ (j = 1 to n) is

$$< a_0^2 e^{i\Delta\phi} >= \frac{1}{n} \sum_{j=1}^{n} \underline{a}_j^*(t) \underline{a}_j(t + \delta t) \tag{2}$$

To improve the accuracy, imagine averaging over a reasonable length of time, say at N time steps $t_1, t_2, \ldots, t_k, \ldots, t_N$, where $t_k = k\delta t$. Then

$$< a_0^2 e^{i\Delta\phi} >= \frac{1}{N} \sum_{k=1}^{N} \left[\frac{1}{n} \sum_{j=1}^{n} \underline{a}_j^*(t_k) \underline{a}_j(t_k + \delta t) \right] \tag{3}$$

We can write this as

$$< a_0^2 e^{i\Delta\phi} >= \frac{1}{N} \sum_{k=1}^{N} \left[\frac{1}{n} \sum_{j=1}^{n} \underline{a}_j^*(t_k) \sum_{j'}^{N} \underline{a}_{j'}(t_k + \delta t) \right], \tag{4}$$

since the cross terms in the square brackets of (4) all involve terms like $e^{-i\omega_j t} e^{i\omega_{j'} t}$, where $\omega_j \neq \omega_{j'}$, and such terms sum to zero when summed over a period substantially longer than their beat period. In fact in the case that the time series is Fourier transformed by a discrete

Fourier transform, all frequencies are harmonically related and so these cross terms summed over the data length are all exactly zero. But the term $\sum_{j=1}^{n} \underline{a}_j(t_k)$ is simply the value of the (complex) time series which would be recorded by the radar at time t_k, which we will denote as $\underline{f}(t_k)$, and so (4) can be written as

$$< a_0^2 e^{i\Delta\phi} >= \frac{1}{N} \sum_{k=1}^{N} \underline{f}^*(t_k) \underline{f}(t_{k+1}) \tag{5}$$

which is simply the autocovariance function at the first lag, $\rho(\delta t)$ say. Thus the mean rate of change of phase can be found from

$$< \frac{d\Delta\phi}{dt} >= \frac{1}{2\pi\delta t} tan^{-1} \left\{ \frac{Im(\rho(\delta t))}{Re(\rho(\delta t))} \right\} \tag{6}$$

where Re means "the real part of" and Im means "the imaginary part of". This estimator of the rate of change of phase was introduced by WOODMAN and GUILLEN, (1974). Notice that the value of the autocovariance $\rho(\tau)$ at $\tau = \delta t$ can also be found from the power spectrum P(f) as (Wiener-Kintchine theorem e.g BRACEWELL, 1978)

$$\rho(\delta t) = \sum_{j=1}^{n} P(f_j) e^{2\pi i f_j \delta t} \tag{7}$$

where $f_j = (j-1)/T$, T being the data length of the time series $\{\underline{f}(t_k)\}$.

Then

$$v_{rad} = \frac{\lambda}{4\pi} < \frac{\Delta\phi}{\delta t} >= \frac{\lambda}{4\pi\delta t} tan^{-1} \left\{ \frac{Im\{\sum_{j=1}^{n} P(f_j) e^{2\pi i f_j \delta t}\}}{Re\{\sum_{j=1}^{n} P(f_j) e^{2\pi i f_j \delta t}\}} \right\}. \tag{8}$$

Since P(f) is real (by definition),

$$v_{rad} = \frac{\lambda}{4\pi} < \frac{\Delta\phi}{\delta t} >= \frac{\lambda}{4\pi\delta t} tan^{-1} \left\{ \frac{\sum_{j=1}^{n} P(f_j) \sin(2\pi f_j \delta t)}{\sum_{j=1}^{n} P(f_j) \cos(2\pi i f_j \delta t)} \right\} \tag{9}$$

In the limit that the term in the right hand brackets {}is is $<< 1$ and the $P(f_j)$ values are small for the larger $\mid f_j \mid$, this approximates to

$$v_{rad} \simeq \frac{\lambda}{2} \frac{\sum_{j=1}^{n} f_j P(f_j)}{\sum_{j=1}^{n} P(f_j)} \tag{10}$$

This last expression is one commonly employed as an estimator of the radial component of the velocity (eg GAGE and BALSLEY, 1978; ZRNIC, 1979). Nevertheless, notice it is only an approximation of the more exact expressions (6) and (9), and breaks down when the argument of the $tan^{-1}\{\}$ expression in (9) becomes comparable to 1. This can happen particularly when the signal is noisy or when the spectral peak is close to the Nyquist frequency, and in these cases the approximation (10) can give erroneous estimates. In the case of high noise levels, the true radial velocity is underestimated. The more exact expressions (6) and (9) will work well in these cases, however.

Some workers extract the radial velocity from the spectrum not by using expressions like (6) - (10), but by fitting a particular spectral shape to the data. Usually a Gaussian function of the type

$$S(f) = N + \frac{P}{\sqrt{2\pi}\sigma} \exp\left[-\frac{(f - f_d)^2}{2\sigma^2} \right], \tag{11}$$

is used, where f is frequency and P, f_d and σ are echo power, mean Doppler shift and root mean square spectral width, respectively. N describes the noise contribution, and represents a constant offset of the spectrum since noise appears with equal spectral density at all frequencies. This method bypasses some of the problems involved in applying equation (10) (e.g. WOODMAN, 1985); its application is fairly straight-forward and it will not be discussed in any more detail here.

2.1.2 Practical problems with the DBS method

Having now determined the radial velocity, it is necessary to determine what it means in terms of atmospheric dynamics. It is generally true that the measured velocity really is the radial component of the mean velocity of the scatterers, but this is not always true, and cases can occur in which the measured velocity is an effective phase velocity of a moving patch. Such cases are rare, but should be born in mind. CROFT (1972) has given an excellent discussion of the Doppler technique, and some of its potential pitfalls.

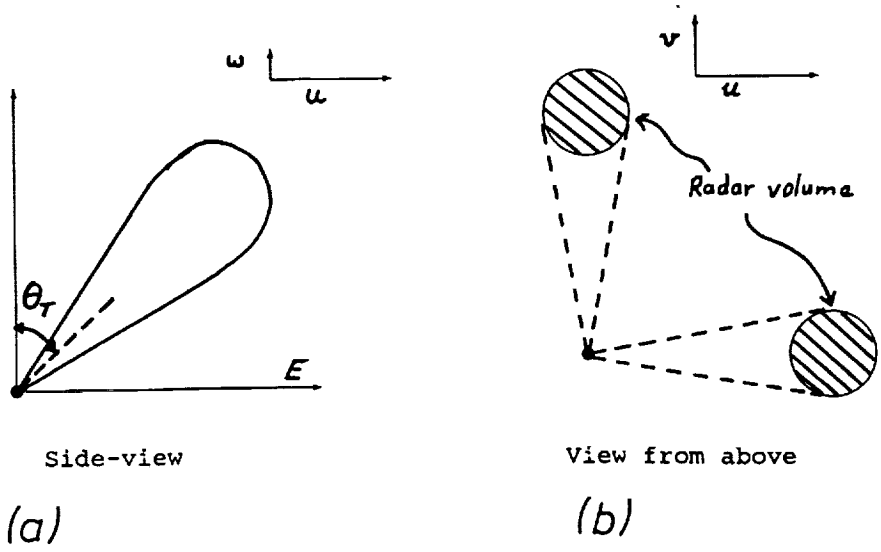

Fig. 3 DBS beam configuration (typical).

There are also many complicating features of a practical nature which arise in using the Doppler method to determine a mean wind (e.g. ROETTGER, 1981). It is sometimes assumed that the vertical wind component is zero, so that off vertical beams can be used to infer the horizontal wind. The situation is described in fig. 3, and if the vertical velocity w is zero then the component of the horizontal wind in the azimuthal direction of the radar v_{hor} can be found as

$$v_{hor} = \frac{v_{rad}}{sin\theta_T} \tag{12}$$

By using orthogonal beams, one say pointing Northward and one Eastward, the total mean horizontal wind can be determined. However, the scatter recorded by each beam is received

from different regions of the sky (fig. 3b), and it is often desirable to know the wind vector at a single point in the sky. Provided that the wind does not vary too much spatially it is possible to assume that both components apply immediately above the radar, but sometimes the divergence of the wind field can be substantial. If the divergence is small, then it is also possible to correct for the vertical velocity, because one can determine the vertical speed w over the radar by using a vertical beam, and then when using an off vertical beam

$$v_{rad} = v_{hor} sin\theta_T + w cos\theta_T \tag{13}$$

so

$$v_{hor} = \frac{v_{rad} - w cos\theta_T}{sin\theta_T} \tag{14}$$

Nevertheless, the possibility of divergences in the wind field is a very real one, and must always be borne in mind when using these expressions.

Even without the problems of spatial variation of the wind field, the above simple assumptions can be in error. For example, if the scatterers are not isotropic, but are on average " stretched out " into horizontally aligned oval-type shapes, then they will have a nonisotropic backscatter polar diagram. Radio waves incident vertically will be more efficiently backscattered than those incident obliquely. Thus for an off vertical beam, strongest scatter will be received from angles nearer to the zenith than from the mean direction of tilt of the beam (e.g. ROETTGER 1981; HOCKING et al., 1986). We might parameterize the backscatter as

$$B(\theta) \propto e^{-\frac{sin^2\theta}{sin^2\theta_s}} \tag{15}$$

and then θ_s is a parameter typifying the nature of the scatterers. For example, θ_s = 90°corresponds to almost isotropic scatter provided we are only interested in angles of θ out to 20°or so, and θ_s = 0°is for the case when reflection only occurs from overhead. (Some authors use the form $e^{-\frac{\theta^2}{\theta_s^2}}$ for $B(\theta)$.)

It can be shown that θ_s relates to the ratio of the length to the depth of the scatterers (HOCKING, 1987a), and this relationship will be discussed in a later section. For the present, we will simply note (e.g see appendix A) that in such cases one should replace the angles θ_T in equations (12) to (14) with the parameter θ_{eff} where

$$sin\theta_{eff} = sin\theta_T \left[1 + \frac{\theta_0^2}{\theta_s^2}\right]^{-1} \tag{16}$$

Here, it has been assumed that the radar two-way polar diagram has a Gaussian shape of the form $exp\{-\sin^2\theta/\sin^2\theta_0\}$ (when aligned vertically), so that the half-power half-width of the beam is $\theta_{\frac{1}{2}} = \sqrt{\ell n 2}.\theta_0$. Even beyond this, however, there are still potential problems with Doppler determination of wind speeds. If there are a variety of shapes, for example, the simple theory of appendix A is not valid. If stratified reflecting steps exist as well as isotropic and anisotropic scatterers, then complications also arise.

The shapes of the scatterers can also affect determination of the vertical velocity. If, for example, the atmospheric scatterers are not aligned exactly horizontally, but have a small tilt, then the direction of preferred scatter will not be immediately overhead, but off to one side. The result is that the small vertical velocities will be contaminated with a small component of the horizontal wind. For example, if the effective tilt is only 1°, and the beam half-power half-width is say greater than about 3°, a horizontal wind of 50 ms^{-1} results in a contribution to the " vertical " velocity of $\sim$ 1 ms^{-1} . This is why most analyses of " vertical velocity

" are made only by using long term means; it is hoped that such tilts average out to zero when averaged over long times, but even then some caution must be exercised. Indeed, a better radar configuration for estimates of the vertical velocity is a bistatic radar, with the transmitter and the receiver well separated (e.g WATERMAN, 1983).

Other problems also exist; for example it is possible that erroneous wind speeds and wind shears will result if the scattering layers are much thinner in depth than the radar pulse-length (e.g. HOCKING, 1983a; FUKAO et al., 1988a, 1988b; MAY et al., 1988)

Despite all these potential problems, the Doppler method still remains a good way to get mean winds in the atmosphere, but any user must be aware of these limitations and bear them in mind during any experimental study.

2.2 Spaced antenna methods: FCA and Interferometer techniques

There are alternative approaches for determining atmospheric wind speeds, and these are the class of spaced antenna methods (e.g. see reviews by HOCKING, 1983c; BRIGGS, 1984; HOCKING et al., 1989). In this, one uses separate groups of antennas, spaced apart on the ground, to determine the wind speed. There are two main approaches ; the first uses cross-correlation techniques to determine the time it takes for the diffraction pattern of the irregularities to cross between groups of antennas, and in its most sophisticated form is called Full Correlation Analysis, or FCA (BRIGGS, 1984). The second approach, originally introduced by PFISTER(1971) and later by FARLEY et al.,(1981), ROETTGER and IERKIC (1985) and ADAMS et al.,(1985) involves using the groups of antennas to form an interferometer. Briefly, such interferometer methods using phase differences between signals received at the groups of antennas to determine angles of arrival. Cross-spectral techniques are used for such angle-of-arrival determinations. Doppler methods are then used to determine the radial velocities associated with each separate scatterer. With such methods, it is possible to calculate the positions of the main scatterers in the sky, hence enabling more accurate determination of horizontal and vertical winds. The major disadvantage of this technique is that it requires that preferred regions of scatter, of narrow angular extent, do indeed exist, so that a direction can be determined. If scatter is diffuse, from a wide range of angles, the method breaks down; even though apparent directions of preferred scatter might still seem to result from the analysis in this case, they are not meaningful (e.g. BRIGGS, 1980).

These two techniques have been discussed extensively in HOCKING et al. (1989), and extensive discussions will not be entered into here. However, it is noted that they are viable and effective alternatives to the DBS method, and their use is growing.

2.3 Brief comments on the various techniques

There are advantages and disadvantages in all these methods. For example, correlation analysis techniques often use small groups of antennas, with corresponding wide polar diagrams. As a consequence, they often produce winds which are averaged over a large area of the sky. On the other hand, there is the advantage that both components of the wind speed are measured in the same volume, directly above the radar. Furthermore, even if the atmospheric scatterers have non-isotropic backscatter polar diagrams, correct estimates of the wind speed still result. The vertical wind speed is not measured, and Doppler methods must be used to determine this.

If isotropic scatterers are the main type of scatter, the spaced antenna and Doppler methods

are equivalent (BRIGGS, 1980). If there is a significant contribution from specular reflectors, it can result in enhanced scatter from the vertical, an advantage for the spaced antenna technique, since that method uses only vertically aligned beams. However, in the extreme that these specular reflector regions form a continuous blanket across the sky, with buoyancy waves causing undulations in this blanket, then the FCA and other simpler versions of the spaced antenna method can break down and effectively measure the phase speeds of the gravity waves. This is a problem for E region studies using MF and HF frequencies, but in the middle atmosphere it is rarely a problem (e.g. HOCKING et al., 1989).

As discussed, the major disadvantage of interferometer techniques is that they require that there are preferred regions of scatter in the sky, of narrow angular extent, so that a direction can be determined. If scatter is diffuse, from a wide range of angles, the method breaks down completely. On the other hand, if such discrete scatterers are present, interferometer methods enable high resolution studies of the scatterers.

It is clear from the preceding discussions that while the principles of estimation of wind speeds are simple, in practice there are many complicating features, and determination of perhaps the simplest target parameters, - their speeds, - is quite complex for the atmospheric case. To first order, all the methods are sound; but if one is interested in details about wind fluctuations, it is clear that it is necessary to know other features of the target, such as their "aspect sensitivity", their shape, the spatial distribution of the scatterers, and perhaps even the cause of the scatterers. In due course, we will address methods to determine such target parameters.

3 Spectral width estimates

So far we have concentrated on determination of mean winds. In the Doppler method, this relates largely to the mean frequency offset of the spectrum, whilst in the FCA method it relates to the time delay of the peak of the cross-correlation function. But there is more information in the signal. In the SA method, the width of the auto and cross-correlation functions holds extra information about the targets; in the Doppler method, the width of the spectrum contains the information. In some ways the second case is easy to visualize, so let us concentrate on this case.

A variety of methods can be used to determine this spectral width. One can utilize either the width of the autocorrelation function where it falls to one half of its value at zero lag, or the second lag of the autocorrelation function, or the second moment of the spectrum (e.g. see the discussion by WOODMAN, 1985). In all cases, one must be careful about the effects of noise, since noise can cause systematic errors. For example, noise produces a narrow spike at zero lag of the autocorrelation function, and this spike should be eliminated before proceeding with analysis. A procedure commonly used to determine the spectral width is least-squares fitting of a Gaussian-like function as in equation (11). In some cases, it is necessary to remove excessively large spikes from the spectra, a procedure which is especially necessary when there are "mirror-like" partial reflectors in the radar volume (e.g. HOCKING, 1983b). The details of these procedures will not be considered here; we are more concerned with the interpretation of the spectral width.

What then can cause the broadening of the spectrum? Perhaps the most obvious is random motion of the scatterers. If each scatterer has a velocity superimposed upon the mean speed, then each produces a line in the spectrum with a different frequency, as illustrated in the following diagram.

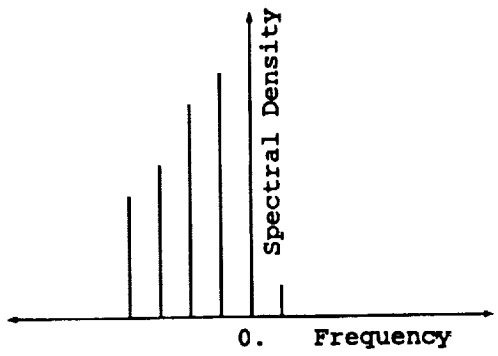

Fig. 4

If the scatterers have, for example, a Maxwellian distribution, then the vertical component of velocity (w) must have a Gaussian distribution, which is proportional to $exp\{-w^2/(2w^2_{RMS})\}$. Since for a vertical beam the Doppler shift from any scatterer is $f = \frac{2}{\lambda}.w$, the spectrum will have a shape of the form $exp\{-f^2/(2f^2_{RMS})\}$, where $f_{RMS} = \frac{2}{\lambda}.w_{RMS}$.

For some years in the early period of VHF middle atmosphere studies, it was assumed that this was the major cause of spectral broadening. However, for most VHF radars, this is not in fact the case. There are other causes of spectral broadening, which while understood by a few (e.g. ATLAS, 1964; SLOSS and ATLAS, 1968; ATLAS et al., 1969; HOCKING, 1983a, b), were not generally appreciated in the Middle Atmosphere community. Fortunately, this attitude has changed recently. These effects will now be discussed.

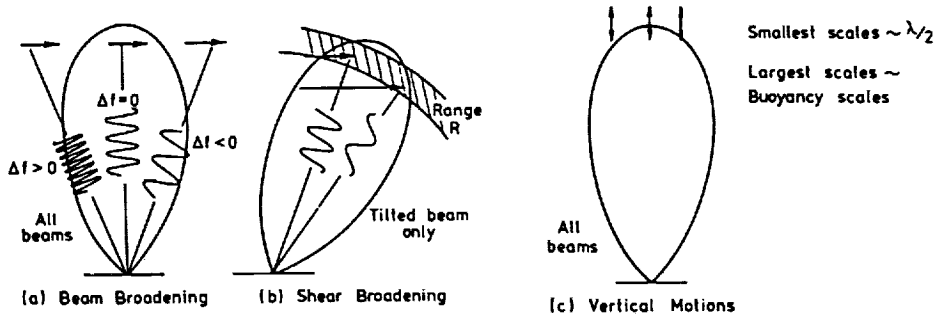

Fig. 5 **Contributors to the spectral broadening at any instant.**

For a vertically pointing beam, probably the main cause of the non-zero spectral width is

the so-called "beam broadening", which is illustrated in fig. 5a.

Even if all the scatterers are moving horizontally at the same velocity, each scatterer will produce a different Doppler shift. The nett result is a spectrum of finite width. This spectral broadening has been modelled by several workers (e.g. HITSCHFIELD and DENNIS, 1956; ATLAS, 1964; SLOSS and ATLAS, 1968; ATLAS et al., 1969; HOCKING, 1983a, b) , and for relatively narrow beams ($\leq$ about 5 °half-power half-width), the spectral half-power half-width $f_{\frac{1}{2}b}$ obeys the approximate relation (in units of Hz)

$$f_{\frac{1}{2}b} = \frac{2}{\lambda}(1.0) \mid \underline{V}_{hor} \mid \theta_{\frac{1}{2}} \tag{17}$$

where $\theta_{\frac{1}{2}}$ is the two-way half-power half-width of the polar diagram in radians, and $\underline{V}_{hor}$ is the TOTAL horizontal wind vector. The same approximation is also fairly accurate even for off-vertical beams, but it is important to note that the TOTAL wind speed should be used, and NOT just the component parallel to the tilt direction of the beam. This formula is based on the assumption that the scattering is statistically isotropic, an assumption which we will relax shortly. When one compares the spectral half-widths due to the non-fluctuating components of the wind-field to the experimental spectral half-widths measured with the vertical beam, one frequently finds that the two are very similar. For example,figure 6 from HOCKING (1983) shows an almost 1:1 relationship between the two parameters when spectra produced from 11s data sets were used.

This point cannot be emphasized too strongly:- the spectral widths are often dominated by so called beam broadening.

There are other effects which alter the spectral width, particularly if the beam is tilted from the vertical. Horizontal fluctuating motions will alter the spectral width (e.g. see fig. 7), and so will changes of the mean wind with height, as occurs for example in a wind shear (e.g. fig 5b). The former effect always broadens the spectrum, whilst the latter one can either reduce or increase the spectral width depending on the sign of the wind shear. These points are discussed in more detail by HOCKING (1983a), for example.

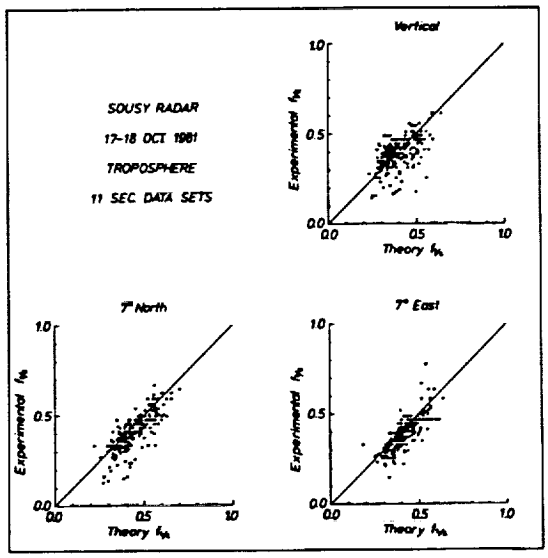

Fig. 6.

Scatter plots of experimental spectral half-power half-widths determined from 11 s data sets vs. the spectral half-width expected purely due to beam and wind-shear spectral broadening for the troposphere.

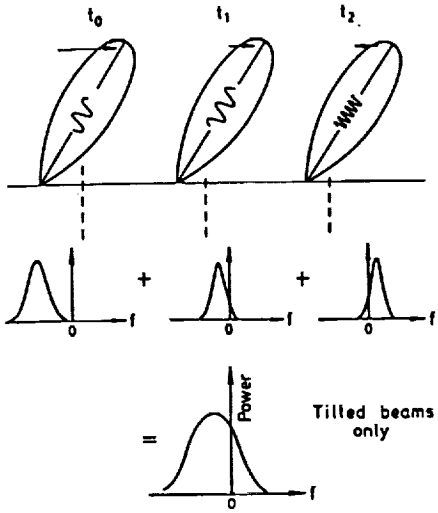

Fig. 7

Illustration of spectral broadening by variation of horizontal wind with time.

Of course the target parameter which is desired is the RMS fluctuating velocity of the scatterers, but this often contributes only a small fraction to the total spectral width. To determine the RMS fluctuating velocity, one should first use the measured mean wind speeds as a function of height, and the known polar diagram (radiation pattern) of the radar, to determine the spectral half-power half-width $f_{\frac{1}{2}nf}$ contributed by the non-fluctuating effects. Then the contribution from the fluctuating component f_{fluct} can be found through the relation

$$f^2_{fluct} = f^2_{\frac{1}{2}expt} - f^2_{\frac{1}{2}nf} \tag{18}$$

This arises because the experimental spectrum is approximately a convolution between the spectrum which would be produced if there were no fluctuating components, and the spectrum due to the fluctuating components alone (at least for very narrow beams ($\leq$ about 5°half-power half-width); the more general case has been modelled by HOCKING, 1983a).

To properly consider all the contributions from the mean wind including wind shear, a more accurate computer model needs to be used (eg HOCKING 1983a), but in many cases equation (17) serves as a useful approximation to obtain $f_{\frac{1}{2}nf}$.

Of course equation (17) is only a first-order estimate of the spectral half-width due to the non-fluctuating component, and it also assumes that the scatterers scatter isotropically. If the scatterers are anisotropic, as may be the case and as has been discussed previously, then the true contribution from non-fluctuating components will be less than that calculated with (17). That equation can still be used, but (see appendix A) $\theta_{\frac{1}{2}}$ must be replaced by $\theta'_{\frac{1}{2}} = R.\theta_{\frac{1}{2}}$ where

$$R = \left[1 + \frac{\theta^2_{\frac{1}{2}}}{\theta^2_{s\frac{1}{2}}}\right]^{-\frac{1}{2}}, \tag{19}$$

$\theta_{\frac{1}{2}}$ being the true half-power half-width of the radar beam, and $\theta_{s\frac{1}{2}}$ is the half-power half-width of the polar diagram of backscatter due to the scatterers (i.e. $\theta_{s\frac{1}{2}} = \sqrt{ln2}.\theta_s$, θ_s being defined by equation (15)). Notice that once again it is important to know the backscatter polar

diagram due to the scatterers, and it is becoming more and more important as we proceed through this text to know this parameter.

Having now determined the contribution due to non-fluctuating aspects of the wind field, and removed it from the experimentally determined spectral half-width, it is now necessary to decide what this residual contribution means, and how to interpret it. There are at least 3 possible contributions to this remaining contribution to the spectral width, namely the effects of fluctuations in the velocity due to turbulence, fluctuations due to buoyancy waves, and the decorrelation time associated with the decay of turbulent eddies. It is not always easy to separate out these terms.

In the case of a vertical beam, the most important effects are the vertical fluctuating component of the turbulent velocity, and both the vertical and horizontal components of the buoyancy-wave field. The horizontal component of the buoyancy field is important because although the beam is vertical, if the wave amplitudes are substantial the radial components of velocity fluctuations occurring near the edge of the beam may still contribute to the spectral broadening. This is especially true when wide beams are used, and is an argument for the use of narrow beams when studies of turbulence are made.

When off-vertical beams are used, both the vertical and horizontal fluctuating components of the turbulent velocity field are important. However, the horizontal components of the buoyancy-wave field become even more important in contributing to the spectral broadening; variations of velocity due to buoyancy waves occur both as a function of position within the radar beam and also as a function of time during the period of data collection. This latter effect can be quite dominant, and swamp the contribution due to the turbulence. For example, fig. 8, taken from HOCKING (1983b) illustrates this point, and shows the dramatic increase in spectral width recorded when an off-vertical beam is used as compared to a vertical beam. In this case the radar was an MF radar observing the mesosphere, and the beam-width was wider than for many VHF radars (about 4.5 °half-width); data were collected for 12 mins in order to emphasize the effect. In normal VHF experiments the effect may not be so dramatic, but nevertheless occurs.

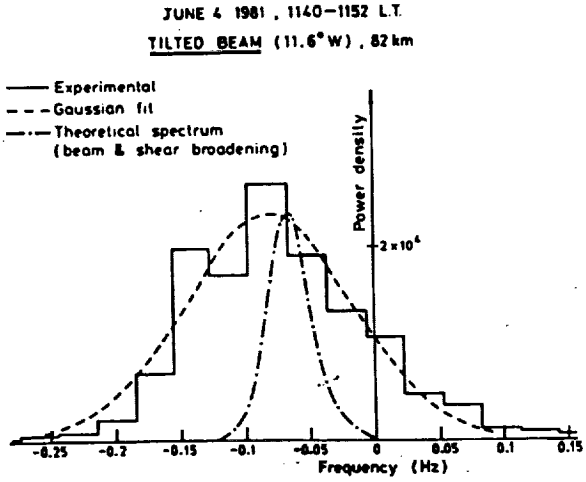

Fig. 8: The solid curve shows a spectrum recorded with the Buckland Park 1.98 MHz radar, using a 10 min data length and a beam tilted 11.6°off-vertical. The dash-dot curve shows the approximate shape of the spectrum recorded with a vertically pointing beam at the same time.

Thus measurements of turbulent energy dissipation rates are best made using a vertical beam. The contribution due to turbulence can be envisaged as follows, and is illustrated in fig. 9. Backscatter occurs predominantly from scatterers with scales of the order of the radar half-wavelength, but these scatterers are carried around by the larger scales. The mean square fluctuating velocity measured by the radar is then the integrated effect from scales of the order of the radar half-wavelength out to scales comparable with the radar volume (e.g SATO and WOODMAN, 1982; HOCKING, 1983a).

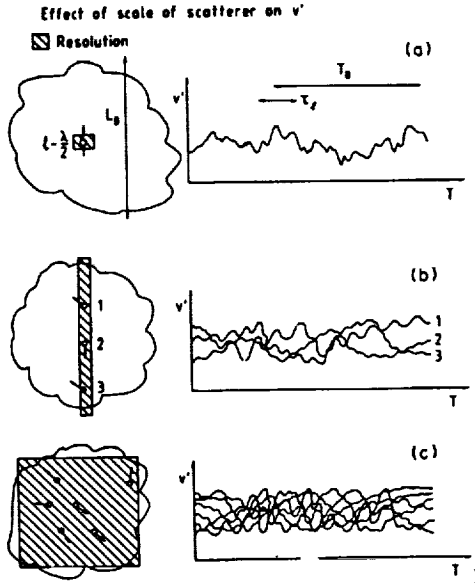

Fig. 9 Illustration of the effect of scale of resolution on measured $\overline{v'^2}$ values. (a) The motion of a single scatterer. In any time interval τ_h only a limited amount of velocity fluctuation occurs, but in the larger time interval T_h the full possible range of velocity fluctuations occur, as larger scales become more effective. (b) and (c) show that many scatterers contribute to the final signal received, each with a different velocity, so a full range of Doppler velocities is experienced in a very short time.

For radars with pulse lengths and beam-widths comparable to the buoyancy scale of turbulence, scales even beyond the buoyancy scale may contribute to the mean square fluctuating velocity, although fortunately with reduced contributions. Let us say that the measured mean-square fluctuating velocity is due to a fraction F from scales within the inertial range of turbulence, and the remaining contribution comes from scales within the buoyancy range. The exact value of F depends on the radar configuration, sampling time, etc., and for the present we will not concern ourselves with its evaluation.

Then we may write (following HOCKING 1983a, 1986) that the velocity variance observed with the radar is

$$\overline{v^2} = \int \Theta_{11}(k_1) dk_1 \tag{20}$$

where $\Theta_{11}(k_1)$ is the longitudinal one-dimensional spectrum function (e.g.BATCHELOR, 1953, p.50) for the direction radial from the radar. The integration is performed over all scales which can affect the radar measurements, which for VHF radars means scales out to the radar pulse length or the buoyancy scale of turbulence, whichever is larger. For a radar pulse length of 600 m, say, this means that scales well into the buoyancy range will be effective, since the thicknesses of these layers is often well below 600 m (e.g. CRANE, 1980; BARAT, 1982) and

the inertial range-buoyancy range transition scale is usually several times less than the layer thickness (e.g. BARAT, 1982). If it is assumed that a fraction F of the measured velocity variance resides in the inertial range and the rest in the buoyancy range, we may write that the measured velocity variance $\overline{v^2}$ obeys the relation

$$\int_{-k_\lambda}^{-k_B} \Theta_{11}(k_1)dk_1 + \int_{k_B}^{k_\lambda} \Theta_{11}(k_\lambda)dk_1 = F.v^2 \tag{21}$$

where k_B is the wave number of the buoyancy scale (transition scale between the inertial and buoyancy ranges) and k_λ is the Bragg backscatter wave number. For Kolmogoroff, inertial-range turbulence, and defining the turbulent energy dissipation rate as ϵ, we may take

$$\Theta_{11}(k) = .1244 C_v^2 \epsilon^{2/3} \mid k \mid^{5/3} \tag{22}$$

and solve for ϵ in terms of k_B, k_λ, and $\overline{v^2}$. C_v^2 is well known from careful atmospheric experiments (e.g. CAUGHEY et al., 1978) to be close to 2.0.

This may then be used (e.g HOCKING, 1983a) to derive

$$\epsilon = \epsilon_* L_B / \left(L_B^{2/3} - \left(\frac{\lambda}{2} \right)^{2/3} \right)^{3/2} \tag{23}$$

where

$$\epsilon_* = 2\pi \left(\frac{F}{.3732 C_v^2} \right)^{3/2} \left(\overline{v^2} \right)^{3/2} / L_B. \tag{24}$$

If F is taken to be 0.5 and $C_v^2 = 2.0$, then we can write approximately that

$$\epsilon = 3.45 \left(\overline{v^2} \right)^{3/2} / L_B. \tag{25}$$

WEINSTOCK (1978b) has suggested that the Buoyancy scale relates to the Brunt-Vaisala frequency and the energy dissipation rate through the relation

$$L_B = \frac{2\pi}{0.62} \epsilon^{\frac{1}{2}} \omega_B^{-\frac{3}{2}}$$

and using this relation with equation (24) gives

$$\epsilon = \left[\frac{12.24F}{C_v^2} \right] \overline{v^2} f_B, \tag{26}$$

f_B being the Brunt-Vaisala frequency in Hz. Again taking $F = 0.5$ and $C_v^2 = 2.0$, we may write

$$\epsilon \simeq 3.1 \overline{v^2} f_B \tag{27}$$

Notice that this also means that

$$L_B \simeq 1.1 \frac{\overline{v^2}^{\frac{1}{2}}}{f_B},$$

a useful relation for making radar estimates of the Buoyancy scale.

Of course $\overline{v^2}$ can be found from the relation

$$\overline{v^2} = f_{fluct}^2 / (2\ell n 2) \tag{28}$$

provided of course that $f_{\frac{1}{2} fluct}$ can be shown to be entirely due to the turbulence.

If F actually varies up to 1.0 or down to 1/4, then the estimates represented by equations (25 and 27) will be incorrect by a factor of 2-3.

These formulae assume that the scattering scale $\lambda/2$ lies in the inertial range. However, it should be noted that if scatter occurs from the viscous range, as may at times happen in the mesosphere, the formulae are still largely valid. It will be noted from (21) that the mean square velocity is an integrated effect due to all scales between $\lambda/2$ and L_B and this integration is dominated by the large scales. A change in the spectral form from (22) within the viscous range will not greatly affect the integral; at worst, the $\lambda/2$ term in (23) may need to be replaced with the inertial range inner scale.

When the radar volume has dimensions less than the buoyancy scale of turbulence, the formula becomes slightly modified. The parameter L_B is replaced by the larger of the pulse length and the radar beam-width at the height of scatter (which we will denote as L_r), and the constant of proportionality changes slightly. In this case k_B in equation (21) is replaced by a Fourier scale representative of the range of Fourier components in the pulse (or the beam-width, whichever is larger). For example, if the pulse is Gaussian in shape with a half-power half-width L_r, then its Fourier transform has a half-width at half-power of about $0.44 \text{x} 2\pi/L_r$. This different situation means that for $L_r \ll L_B$, the following relation applies (e.g. LABITT, 1979; BOHNE, 1982 (appendix C))

$$\epsilon \simeq 1.3 \left(\overline{v^2}\right)^{3/2} / L_r. \tag{29}$$

The constant (1.3) has changed considerably compared to that in (24) and (25), and there are two main reasons for this. Firstly, the constant 1.64 assumes that there is no Buoyancy scale, and assumes that the $k^{-\frac{5}{3}}$ law applies over all scales; thus Fourier scales of small wavenumber, although only a small contribution to the pulse, make a large contribution to the integral in (21). As a result, (29) should not be applied even if L_r is less than but comparable to L_B; in that case, the constant to be used should be considerably larger. The second reason relates to the different physical significances of L_r and L_B.

It should also be noted that even if $L_r \ll L_B$, if data lengths of a minute or so are used in forming the power spectra, equations (24) and (25) are better estimators of ϵ; see fig. 9.

The relations (23-29) (whichever is applicable) may be used to determine the turbulent energy dissipation rate if one knows the contribution to the spectrum from turbulent fluctuations. However, we still must decide whether all the remaining spectral width is indeed due to turbulent fluctuations. Even when vertical beams are used to measure the spectrum, there may still be a small contribution due to buoyancy waves, (as has already been discussed), but it is possible to make at least some attempt to separate the turbulent and buoyancy wave effects. Use of procedures which involve least-squares fitting to a Gaussian shape like (11) help, because buoyancy-wave fluctuations of specular reflectors, for example, can produce fairly non-Gaussian spectra. Thus spectra dominated by buoyancy-wave fluctuations are often rejected by such procedures. Another possibility is that used by HOCKING (1988),who utilized the fact that the buoyancy-wave field tends to have only a small contribution (if at all) from oscillations with periods of less than 5 min. This is not to say, however, that using a data length of less than 5 mins eliminates the wave effects, since even a fraction of a wave cycle could cause significant contributions to the spectral width. However, one can predict how the spectral width might change as a function of data length in this case, and by comparing this prediction to the true variation in spectral width as a function of data length, can make some estimate of the relative contributions of buoyancy waves and turbulence. Such a process has some uncertainty associated with it, but is nevertheless of some value. An example was given in HOCKING (1988).

We have not yet addressed the contribution due to the decorrelation time associated with the finite lifetime of the eddies. In fact provided that the radar wavelength is substantially less than the buoyancy scale, this is not a major contribution, as will now be shown.

If the energy dissipation rate is again denoted ϵ, the typical eddy scale as ℓ and the velocity associated with such an eddy is denoted as v, then the typical lifetime τ of an eddy is

$$\tau \sim \frac{\ell}{v} \tag{30}$$

where

$$\epsilon \sim \frac{v^2}{\tau}. \tag{31}$$

Hence

$$\tau \sim \frac{v^2}{\epsilon} \sim \left(\frac{\ell}{\tau}\right)^2 . \frac{1}{\epsilon} \tag{32}$$

so that

$$\tau \sim \ell^{\frac{2}{3}} \epsilon^{-\frac{1}{3}} \tag{33}$$

Thus the growth and decay of eddies prduces an autocorrelation function with a half-width at a value of 0.5 of about τ , where τ is given by the above expression. If the autocorrelation function is taken to be Gaussian, then its Fourier transform is also Gaussian, with a half- power half-width of 0.22 / τ, and we will denote this as f_{dc} , where "dc" stands for "decorrelation" Thus

$$f_{dc} \simeq \frac{.22}{\tau} \sim .22 \ell^{-\frac{2}{3}} \epsilon^{\frac{1}{3}}, \tag{34}$$

where ℓ can be taken to be of the order $\lambda/2$.

Contrast this to the contribution due to fluctuating motions, which contribute out to scales of the order of the Buoyancy scale, L_B. In this case, we have already seen (equation 25) that if we take F as about 0.5, then

$$\epsilon \simeq 3.5 \frac{v_{RMS}^3}{L_B}. \tag{35}$$

Then the half-power half-width of the spectrum due to the fluctuating motion of the scatterers is given by

$$f_{fluct(m)} \simeq .8 \left(\frac{2}{\lambda}\right) \epsilon^{\frac{1}{3}} L_B^{\frac{1}{3}} \tag{36}$$

Hence the ratio of spectral half-widths due to the eddy motions and the decorrelation time of the eddies is

$$\frac{f_{fluct(m)}}{f_{dc}} \sim 4 \left[\frac{L_B}{\lambda/2}\right]^{\frac{1}{3}} \tag{37}$$

Physically this arises because the spectral width associated with the scatterer movement is related to the buoyancy scale L_B, (since we have seen that this width is due to the integrated efect of all scales up to L_B), whilst the decorrelation time depends only on the scale of the scatterers.

For a typical case with $\lambda/2$ equal to 3m, and L_B equal to say 200 m, the ratio is about 16. Since the total spectral width due to these two components combined is equal to the square root of the sum of the squares, the correction due to the decorrelation time in this case would be only a fraction of a percent. Thus provided the Buoyancy scale is greater than the Bragg

backscatter scale by a few times, the decorrelation time of the eddies is only a minor correction to the spectral width and can usually be ignored.

It was mentioned earlier that information about the level of turbulence also exists in the correlation functions, and can be obtained from the Full Correlation Analysis technique using spaced antennas. Indeed, one of the output parameters of the Full Correlation Analysis is a parameter which is usually denoted as $T_{\frac{1}{2}}$ and represents the correlation function half-width which would be measured with a radar which moved along the ground with the velocity of the mean wind in the scattering region. Spectral beam-broadening has been removed from this parameter, although the effects of wind-shear have not. Thus the parameter $f_{\frac{1}{2}} = 0.22/T_{\frac{1}{2}}$ can be used in place of f_{fluct} in all the discussions above; the main potential problem is that there may be increased contributions from buoyancy waves if the polar diagram of the system is wide.

Provided the effects of gravity waves can be adequately separated, or even shown to be relatively unimportant, the procedures described above allows radars to be used to extract estimates of atmospheric turbulence.

It is also possible to infer the turbulent diffusion coefficient for a turbulent layer through the relation

$$K_M = c_2 \epsilon / \omega_B^2 \tag{38}$$

e.g. WEINSTOCK, 1978a, b; LILLY et al. 1974). The constant c_2 is quoted to have a variety of values in the literature, ranging from about 0.25 to 1.25. The most commonly accepted value seems to be 0.8 (WEINSTOCK, 1978). Ideally it is also necessary to know the Brunt-Vaisala frequency averaged over the turbulent layer, but unfortunately it is not always possible to find this. Some authors use climatological values, but it is better to use radio-sonde determinations where possible.

The method of determining ϵ described above has been used a few times, but is still largely unexploited; a much greater use of these procedures is to be actively encouraged.

4 Power Measurements

One simple but effective method for deducing information about the scatterers is to record the backscattered power. In many experiments powers are compared in a relative way; for example, power variations as a function of time and height are usually studied in most experiments. Even this simple process can give useful results, but it is even more effective if the radar can be calibrated in an absolute sense. This requires some careful work by the user, but if this is done it is then possible to convert the measured powers to effective reflection coefficients, backscatter cross-sections, or perhaps estimates of the turbulence intensity. (The parameter actually calculated depends largely on the scattering mechanism, and we will consider ways of determining this shortly.) Such calibration not only allows better comparisons to be made world-wide, but also allows better comparison with theory.

Before showing how this calibration can be done, however, it is a useful exercise to look in more detail at the mathematical formulation of the scattering process. We will begin by considering the simplest case, namely that of reflection from stratified steps.

4.1 Modelling the reflection and scattering processes

4.1.1 Horizontally stratified structure

Consider first, and for simplicity, a horizontally stratified atmosphere which has fluctuations in the refractive index in the vertical direction but none horizontally. In fact we will see later that this is not such an unreasonable model, and has some real applicability in the atmosphere. A pulse of the form $g_1(t-z/c)cos[\omega_c(t-z/c)]$ is transmitted, where $f_c = \omega_c/(2\pi)$ is the carrier frequency. At $z = 0$, this is a pulse which varies in time as $g_1(t)cos(\omega_c t)$. This can be written as $g(\xi) = g_z(\xi)cos(k\xi)$ where $k = 2\omega/c = 4\pi/\lambda$ (λ being the radar wavelength) and $\xi = ct/2$ is a length coordinate which closely matches the height of the scatterers (e.g. HOCKING and ROETTGER, 1983). If the refractive index fluctuations are described by $n(z)$, then the radio-wave reflection coefficient profile is given approximately by $r(z) = \frac{1}{2}(dn/dz)$ (eg HOCKING and VINCENT, 1982a). The reflected complex amplitude as a function of height is then given by

$$a(z) = \{\frac{r(z)}{z}\} \otimes g(z) \tag{39}$$

where $\otimes$ stands for convolution. (e.g HOCKING and ROETTGER, 1983, and references therein). (This expression is very accurate for VHF scatter, although if absorption is high or the pulse is significantly dispersive, more careful approaches are necessary, such those given by HOCKING and VINCENT (1982b), or even full-wave equations are necessary (e.g. BUDDEN, 1965).)

To begin, it is of interest to examine what happens when reflection occurs from a single step of some finite thickness. The easiest step to deal with is one of the type with

$$r(z) \propto e^{\{-\frac{(z-z_0)^2}{d^2}\}}. \tag{40}$$

In this case the refractive index profile is a step of finite thickness, as shown in the following diagram. Note that although d is a measure of the step depth, it is probably not the best measure of this depth. A better measure of the step depth might be the distance between the two points where the reflection coefficient falls to one half of it maximum value, or

$$w = 2\sqrt{ln2}.d$$

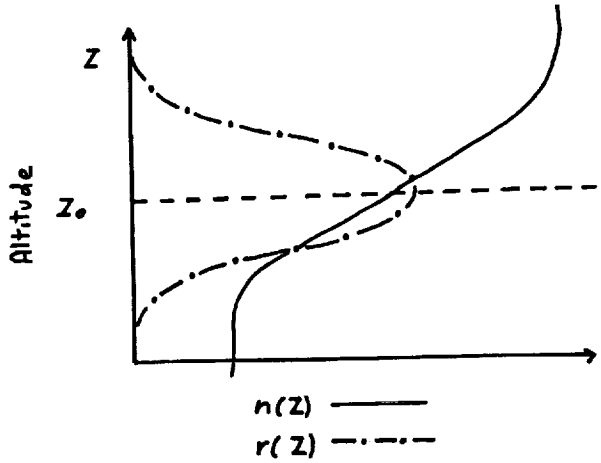

Fig. 10

The convolution can be done numerically, but it is instructive to examine the process using a slightly different approach. From Fourier theory (e.g. BRACEWELL, 1978) the convolution can be done by Fourier transforming each of $g(z)$ and $r(z)$, multiplying the Fourier transforms $G(k)$ and $R(k)$, and then re-Fourier transforming the product. The process is illustrated diagramatically in the following diagram.

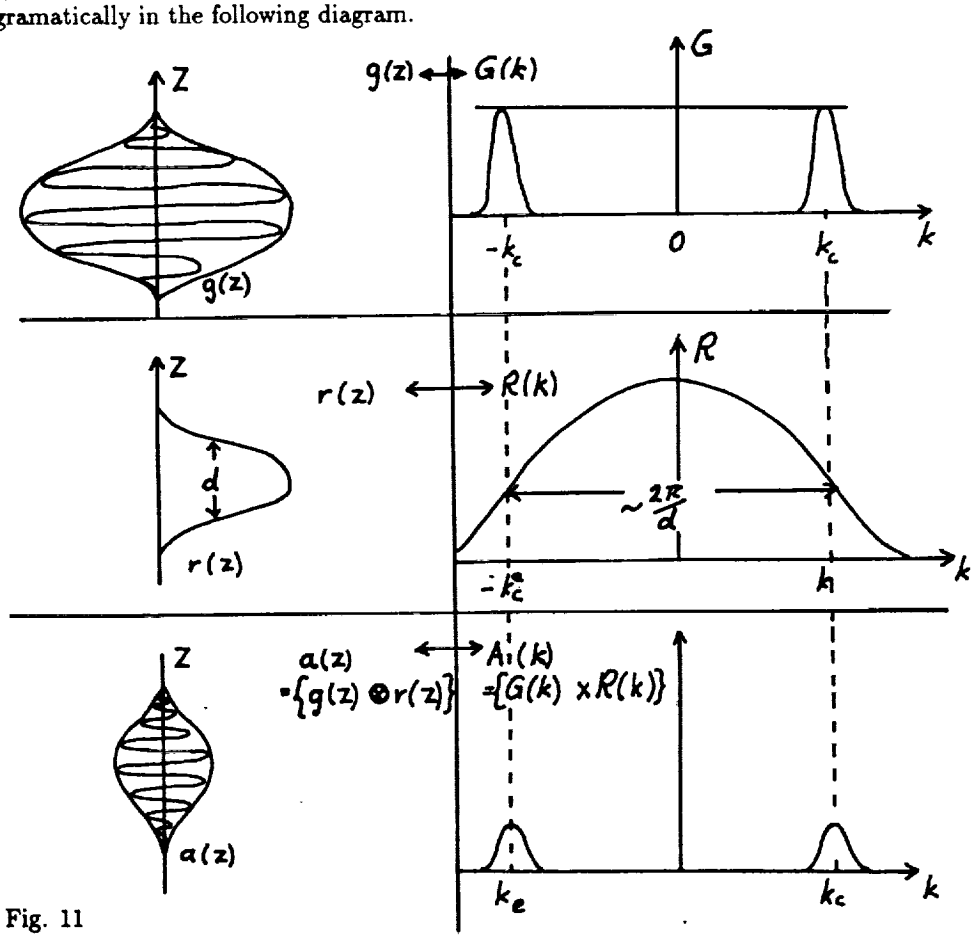

Fig. 11

Note that the Fourier transform $G(k)$ of $g(z)$ exists in a narrow band centred at $k_c = 4\pi/\lambda$. Notice also that the narrower the step (smaller d) the wider the function $R(k)$ and so the product of the Fourier transforms is larger. In fact the peak amplitude of the product is

$$A(k_c) \propto e^{-\frac{k_c^2 d^2}{4}} \propto e^{-\frac{4\pi^2 d^2}{\lambda^2}} \tag{41}$$

- so clearly once d exeeds λ, the backscattered power is very small. In fact even if $d = \lambda/4$ ($w = 0.42\lambda$), the reflected amplitude is 0.08 times that for a step of zero width (ie a sharp discontinuity). The power will therfore be reduced by 22 dB compared to a single step. Many authors have taken this to infer that only steps much less than about a quarter wavelength in thickness will ever be seen by radar, and this may well be true for say MF radars. However, with coherent integration and the greater sensitivity of modern radars, particularly VHF radars, it is not so easy to adopt this argument; VHF radars can often see such steps even if reduced in efficiency by 20 dB, and they are indeed capable of detecting layers with a depth d of about

$\lambda/4$. However, it is true that beyond this depth, the efficiency falls off remarkably quickly; for example, if $d = \lambda/2$, the power is reduced by 80 dB, and even VHF radars would not normally detect such a step. HOCKING (1987a) has discussed this point and suggests that some "specular reflectors" seen by VHF radars have typical depths with $2d$ = 3 - 4 m, or w between 2.5 and 3 metres; in other words, the steps are right on the edge of the region of detectability.

Another useful model is that of "Fresnel Scatter", a model known for many years in D region MF studies, (eg AUSTIN et al., 1969; MANSON et al., 1969; GREGORY and VINCENT, 1970), but given renewed popularity by GAGE et al (1981) in respect to VHF studies. In this model, horizontal stratification is again assumed, but $n(z)$ is assumed to vary randomly, so the atmosphere can be thought of as a series of thin slabs sitting atop each other, each with slightly different refractive indices. Despite some initial controversy, it is relatively easy to show that in this case the backscattered power is proportional to the pulse length (HOCKING and ROETTGER 1983), and if one includes the decrease in reflected power as a function of height z then one finds that the power received by a radar takes the form

$$P_R = \frac{\alpha^2 P_t A_e^2}{4\lambda^2 z^2} \left[F(\lambda)\overline{M}\right]^2 (\Delta z) \tag{42}$$

where P_R is the received power, α is the array efficiency, P_t is the peak transmitted power, A_e is the array effective area, λ is the radar wavelength, z is the height of reflection, $\overline{M}$ is the mean generalized refractive index gradient and $F(\lambda)$ is a "calibration constant" which must be determined empirically for each radar. The term Δz represents the radar pulse-length. In the case that $\overline{M}$ varies substantially within one pulse-length this formula need some modification, as described by HOCKING and ROETTGER (1983). Later developments of this model have been discussed by GAGE et al., (1985) and GREEN and GAGE, (1985).

4.1.2 Three dimensional structures

The next extension to these models is to allow the scattering medium to have non-constant structure in the horizontal direction as well. An example might be fully developed isotropic turbulence, in which the refractive index has random fluctuations caused by the turbulent velocity field. In this case, the theory for relating the backscattered signal to the turbulence intensity has been fairly well developed (OTTERSTEN, 1969; VANZANDT et al, 1978; HOCKING, 1985). The backscattered power depends not only on the intensity of the turbulence, but also the mean refractive index gradient in which the turbulence exists. In the mesosphere, the latter term is largely determined by the electron density gradient, in the stratosphere by the temperature gradient, and in the troposphere by the temperature and humidity gradient. Expressions for these potential refractive index gradients are given below, but expressions for evaluation of the turbulence intensity from measurements of the absolute backscattered power wil be left until after the following section on calibration of a radar.

In the unionized atmosphere, and for centimetre and metre radio waves, the potential refractive index gradient is given by (TATARSKI, 1961, p 57)

$$M = \frac{-79 \times 10^{-6}}{T^2}.P.\left[1 + \frac{15500}{T}q\right]\left[\frac{dT}{dz} + \Gamma_a - \frac{7800}{1 + \frac{15500}{T}q}.\frac{dq}{dz}\right], \tag{43}$$

where P is the atmospheric pressure in units of millibars (hPa), T the temperature (°C), Γ_a is the adiabatic lapse rate, and $q = e/(1.62P)$ is the specific humidity, e being the water vapour pressure.

In the ionosphere, the relevant potential refractive index gradient is given by (HOCKING, 1985)

$$M_e = \frac{\partial n}{\partial N}\left[N\frac{\omega_B^2}{g} - \frac{dN}{dz} + \frac{N}{\rho}\frac{d\rho}{dz}\right] \tag{44}$$

where N is the electron density, n is the refractive index, and ρ is the neutral density of the atmosphere. The Brunt-Vaisala angular frequency is represented by ω_B^2, and g represents the acceleration due to gravity. Notice that this can also be written as (e.g. THRANE and GRANDAL, 1981)

$$M_e = \frac{\partial n}{\partial N}\left[\frac{N}{\gamma P}\frac{dP}{dz} - \frac{dN}{dz}\right] \tag{45}$$

where γ is the ratio of specific heats at constant pressure and constant volume.

For a VHF radar,

$$\frac{\partial n}{\partial N} = \frac{1}{2}\pi^{-1} r_e \lambda^2, \tag{46}$$

where r_e is the classical electron radius. At HF and MF, the relation between N and n becomes more complex (e.g. BUDDEN, 1965).

Let us now turn our attention to the subject of calibrating the radar, so we may then see how to use the above expressions to determine turbulence intensities.

4.2 Calibration of the radar

In order to calculate the parameters like backscatter cross-sections of the scatterers or the reflection coefficients of the reflectors, it is necessary to calibrate the radar. In this context, "calibration" refers to calculation of appropriate coefficients which enable conversion between the power received by the radar and reflection coefficients, back-scatter cross-sections etc (rather than determination of the polar diagram of the radar, for which the term "calibration" is also often used). Many radars world wide have still not been absolutely calibrated, which is a great pity.

One simple way of "calibrating" the measurements is to compare the signal received to the noise. For a VHF radar, the noise is predominantly sky-noise, due to extra-terrestrial sources. By measuring the ratio of the signal-to-noise (S/N), it is possible to get an approximate measure of the received power, provided the noise level is known (e.g. VANZANDT et al., 1978). Standard charts exist which may be used to give the noise level. However, this is not the best way to determine the signal power. For example, the true noise level has a diurnal variation, depending on the passage of noise sources through the beam, and of course radars at different locations have different dominant noise sources . It is also likely that the noise level may change as one changes the orientation of the beam. Furthermore, the procedure is of no use for MF and HF systems, in which noise depends on atmospherics like lightning. Therefore, other more accurate calibration procedures are to be preferred.

A moderately effective technique is to use a noise generator to calibrate the receiver. A noise generator is fed into the receivers at the point where the receiving antennas are normally connected, and the signal is recorded. Usually VHF radars employ coherent integration of the signal, and of course noise is incoherent, and this factor must be taken into account when the calibration is performed. For noise, the sum of N coherent integrations increases the total power by factor of N times, whilst for coherent signal it increases by a factor of N^2. These differences are usually fairly easy to allow for, however, and calibration in this way is relatively simple (e.g. HOCKING et al., 1983). One simply determines what a particular level of receiver input power produces in terms of output units, and henceforth any measured receiver output

can be converted back to an input noise power. Standard radar equations may then be used to determine parameters like the scatterer cross-sections and reflection coefficients. For example, knowing the output power of the transmitter, P_t, the reflection coefficient of a scattered layer can be found through the relation

$$P_R = \frac{P_t e_t G}{4\pi(2z)^2} e_R A_R . \overline{R^2} \tag{47}$$

where P_R is the received power, P_t is the power produced by the transmitter, G is the gain of the transmitting array, e_t and e_R are the efficiences of the transmitting and receiving systems, (including the efficiencies of the respective arrays), A_R is the receiving area of the receiving array, and $\overline{R^2}$ is the mean square reflection coefficient. In the case that the same array is used both for transmission and reception, we may use the relation $A_R = G\lambda^2/(4\pi)$ to give

$$\overline{R^2} = \frac{P_R 64\pi^2 z^2}{P_t G^2 e_t^2 \lambda^2} \tag{48}$$

If the scatter is due to turbulence, an effective backscatter cross-section σ can be found. Here, σ is the power backscattered per unit solid angle, per unit incident power density, and per unit volume. σ is evaluated through the relation (e.g. HOCKING, 1985)

$$P_R = \frac{P_t e_R e_t G A_R}{4\pi z^4} . \sigma . \frac{V}{\ell n 2}, \tag{49}$$

where V is the radar volume. For a monostatic radar, $V = \pi(z\theta_{\frac{1}{2}})^2 . \Delta z$, where $\theta_{\frac{1}{2}}$ is the radar two-way half-power half-width and Δz is the pulse length ($= c\tau/2$, where τ is the transmitted pulse length in seconds and c is the speed of light in ms^{-1}).

The efficiency e is often hard to determine, but even if $\overline{R^2}$ or σ or C_n^2 can be determined to within a factor of 2 or 3, it is still useful. Various ways exist for calculating radar efficiencies, but lack of space prevents their discussion here. Examples include methods discussed by VINCENT et al., (1986) and MATHEWS et al., (1988).

At HF and MF, use can be made of the fact that the radio pulses are totally reflected from some part of the ionosphere. If a so called "second hop" echo occurs, (which arises when the pulse is totally reflected, returns to the ground, is re-reflected back to the ionosphere and returns), then the ratio of the strengths of the main and second hop echoes may be used to determine a calibration constant for the system. To see this, write that the power received form a reflecting layer at height z, and of reflection coefficient R is

$$P_{1R} = \kappa^{-2} \overline{R^2} z^{-2} P_t . \tag{50}$$

where κ is a calibration constant. In this case, P_t need not even be the actual transmitted power, but any value proportional to it. Then if a second-hop echo exists, the received power from it is

$$P_{2R} = \kappa^{-2} \overline{R^2}^2 (2z)^{-2} P_t . \tag{51}$$

Then squaring (50) and dividing through by (51) allows elimination or $\overline{R^2}$ and so

$$\kappa = \frac{2\sqrt{P_t}\sqrt{P_{2R}}}{z P_{1R}} \tag{52}$$

In this case, neither P_R nor P_t need to be known absolutely, and each can be a quantity which is simply proportional to the true received and transmitted powers. κ can be determined

as above, and then for any echo, whether it be strong enough to have a second hop or not, $\overline{R^2}$ can be evaluated through (50).

In VHF studies, there is no totally reflecting surface. It is possible to use artificial satellites, or even the moon (e.g. MATHEWS et al., 1988) to calibrate the system, provided that the backscatter cross-section of the target is known. In this case, the efficiency terms can also be evaluated.

The absolute calibration of radars by any of the means discussed above, or any other means, is to be actively encouraged, and will make comparisons between radars and between observations and theory much easier in the future.

4.2.1 Determination of turbulence intensities from measurements of received power

Once it can be ascertained that turbulence is the main cause of the radio wave scatterers, it is possible to convert the received powers to parameters which describe the turbulence. One key parameter is the "(potential) refractive index structure constant", usually denoted as C_n^2. If the turbulence obeys the classical Kolmogoroff inertial spectrum, then the spectrum of refractive index fluctuations is given by (TATARSKI, 1961, 1971)

$$\phi_n(k_x, k_y, k_z) = 0.033 C_n^2 \mid \underline{k} \mid^{-\frac{11}{3}} \tag{53}$$

where a normalization has been chosen such that $\int\int\int_{-\infty}^{\infty} \phi(\underline{k}) d\underline{k} =< n^2 >$. Thus C_n^2 is a parameter which indicates the level of refractive index fluctuation. C_n^2 can be determined from the cross-section defined above through the relation

$$\sigma = 0.00655 \pi^{\frac{1}{3}} C_n^2 \lambda^{-\frac{1}{3}} \tag{54}$$

(Note that sometimes a cross-section $\eta = 4\pi\sigma$ is used, in which case $\eta = 0.38 C_n^2 \lambda^{-\frac{1}{3}}$). When combined with the equations seen earlier, we see that for a monostatic radar

$$C_n^2 \approx 66. \frac{P_R z^2 \lambda^{\frac{1}{3}}}{P_t A_R \epsilon_t^2 \Delta z} \tag{55}$$

Appropriate relations can also be easily derived for the case in which the transmitter and receiver are separate systems (also see HOCKING, 1985).

C_n^2 is a useful parameter, but an even more useful one is of course the turbulent energy dissipation rate, ϵ. It is possible to relate C_n^2 to ϵ in the following way.

Starting from TATARSKI, 1961, (p44, equation 3.19), we have

$$C_n^2 = a^2 N \epsilon^{-\frac{1}{3}}, \tag{56}$$

where N is a parameter defined by

$$N = K_n M^2 \tag{57}$$

for a stratified environment. The constant a^2 has been measured to be about 2.8. Using the definition of the Prandtl number $P_r = K_M / K_n$, defining $\alpha' = P_r^{-1}$, and using the relation seen earlier that

$$K_M = c_2 \epsilon / \omega_B^2 \tag{58}$$

e.g. WEINSTOCK, 1978a, b; LILLY et al., 1974), we may see that

$$\epsilon = \left[\frac{C_n^2 \omega_B^2}{a^2 \alpha' c_2 M_n^2} \right]^{\frac{3}{2}} \tag{59}$$

These relations have also been derived by BLIX (private communication, 1988) ; a similar expression was derived by VANZANDT et al., (1978) and noted by HOCKING (1985), although a slightly different proof was used in the second case, with the result that

$$\epsilon = \left[\frac{C_n^2 \omega_B^2}{a^2 \alpha' M_n^2 \left[\frac{R_{i(c)}}{b^2} \right]} \right]^{\frac{3}{2}} \tag{60}$$

$R_{i(c)}$ is the critical Richardson number at which turbulence should develop, and b is yet another constant relating the energy dissipation rate to the mean windshear. In fact VANZANDT et al., (1978) and HOCKING (1985) took b =1.0, so b did not appear explicitly in their expressions, but with hindsight this was not wise. The first expression (59) is derived in a more fundamental way, and requires less assumptions, than the second (60), and it is better to use the former. The constant c_2 is quoted to have a variety of values in the literature, ranging from about 0.25 to 1.25. The most commonly accepted value seems to be 0.8 (WEINSTOCK, 1978b).

An extra complication arises if the turbulence does not fill the radar volume, and indeed this often appears to be the case. It appears that in the stratosphere and mesosphere, turbulence occurs in relatively thin layers with thicknesses ranging from a few tens of metres to perhaps a kilometre or so, but generally of the order of 100m. At any one instant, only a small fraction of the radar volume contains turbulence, and this should be taken into account when calculating ϵ. In other words, the calculated value of C_n^2 is actually too small by a factor F_t, where F_t is the fraction of the radar volume which is filled with turbulence at any one time. Thus one normally calculates

$$C_n^2(turb) = C_n^2(radar)/F_t, \tag{61}$$

where $C_n^2(radar)$ is the value determined from the radar measurements. VANZANDT et al.(1978, 1981) have developed models for the variation of F as a function of atmospheric conditions, enabling estimates of ϵ to be made. Furthermore, one is often interested in the mean value of ϵ averaged over the radar volume, so VANZANDT et al. suggested calculating the quantity

$$\bar{\epsilon} = F_t \epsilon_{turb} \tag{62}$$

GAGE et al. (1980) used a simplified model based on VanZandt's model, in which they showed that the parameter $F_t^{\frac{1}{3}} \omega_B^2$ could be determined to moderate accuracy from climatological data, so that the simplified expression

$$\bar{\epsilon} = \gamma [C_n^2(radar)]^{\frac{3}{2}} [\frac{T^3}{P}] \tag{63}$$

could be used, where $\gamma = 1.08 \times 10^{22}$ for a dry troposphere and $\gamma = 3.25 \times 10^{21}$ for the stratosphere. Here, P is in millibars, T in Kelvin, C_n^2 is in units of $m^{-\frac{2}{3}}$ and ϵ is in units of Wkg^{-1}. Variations on these principles have also been presented by CRANE (1980) and WEINSTOCK (1981).

Further complications arise if the turbulence is not isotropic, but we will not discuss these problems here, important though they are, due to lack of space.

5 Aspect sensitivity of the scatterers

We have seen several times throughout this text that a better understanding about the shapes of the scatterers is necessary in order to better interpret measurements of wind speed and turbulence intensities. It would also naturally help in understanding the cause of the scatterers.

The shape of the scattering irregularities has been the subject of active debate over many years. Models have ranged from flat, mirror-like partial reflectors to "pancake-like" scatterers to inertial-range isotropic turbulence, and in this review we will not dwell too much on these arguments. Rather, we will first describe the main models, and then concentrate on the sorts of techniques which might be, and have been, used to determine the shapes of the scatterers.

If it is assumed that the polar diagram of backscatter of the scatterers is of the form

$$B(\theta) \propto e^{-\frac{\sin^2\theta}{\sin^2\theta_s}} \tag{64}$$

, as assumed in equation (15), then θ_s gives a measure of how rapidly the backscattered power falls off as a function of zenith angle. If θ_s tends towards 90 °, it indicates isotropic scatter, whilst if θ_s tends towards 0°then it indicates highly aspect-sensitive scatter.

There are a variety of models which have been advanced, but they basically fall into 2 categories. (e.g. LINDNER, 1975 a,b; BRIGGS and VINCENT, 1975; ROETTGER and LIU, 1978; GAGE and GREEN, 1978; HOCKING, 1979; FUKAO et al., 1980a, b; ROETTGER, 1980b; GAGE et al., 1981; DOVIAK and ZRNIC, 1984; WATERMAN, 1985, amongst others).

(A) The first class assumes that individual scatterers are (on average) ellipsoidal in shape, which may vary in their length to depth ratio as a function of scale. The extremes are spherical shapes (isotropic scatter) and highly elongated structures.

(B) The second class of model assumes a horizontally stratified atmosphere consisting of variations in refractive index in the vertical direction, so one can think of this as a series of "sheets" of different refractive index. Such structures, if truly stratified, would have $\theta_s = 0$, but if we imagine that these sheets are gently "wrinkled", then θ_s will become non-zero (e.g. RATCLIFFE, 1956). In this case, the range of θ_s values relates to the range of Fourier components necessary to describe the wrinkles.

Proponents of model B do not claim that the whole atmosphere is like this, but that it is like this in some places at some times, and use the model to describe particular observations.

Sometimes hybrids of the two models are invoked and other, more complicated, models have also been proposed, but they are generally based on the above models. To illustrate these later models, as well as give a feel for how they are explained physically, some examples of such more complicated models are shown below. The first (fig. 12a) is due to BOLGIANO (1968), and assumes that an intense turbulent layer might mix the layer so that the potential refractive index across the layer is constant, with sharp edges at the side. These edges might be able to explain the model B reflectors, for example, although doubts about the possibility of a turbulent layer maintaining sharp edges exist.

The second model in fig. 12 proposes that scatterers near the edges of a confined layer of turbulence are more anisotropic than in the centre. The model has been discussed by HOCKING et al. (1984), noted by HOCKING (1985), and also proposed independently by WOODMAN and CHU (1989). Such a model is physically likely because turbulent layers are often more stable near their edges (e.g. PELTIER et al., 1978; KLAASSEN and PELTIER, 1985), but for the purposes of this paper these models are simply noted as the type of extension to the simple models proposed above which should be borne in mind.

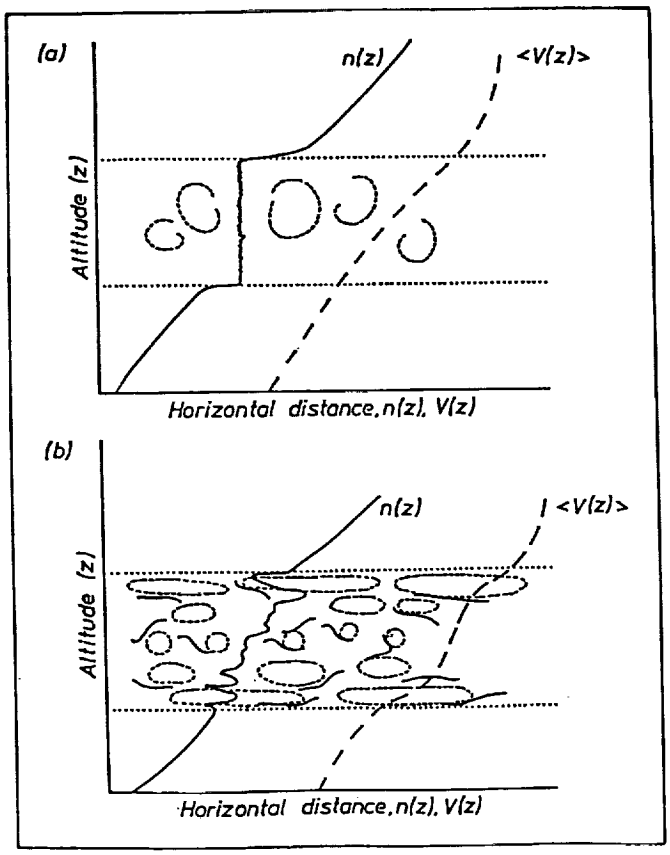

Idealized views of two models for turbulence in the atmosphere. The broken lines represent "eddies", and the solid lines represent scatterering interfaces. The first graph represents an earlier proposal due to Bolgiano (1968), and the second represents a model discussed in the text.

Fig. 12

Another model which may give a physical basis to model B is the proposal that the specular reflectors might be damped gravity waves (e.g. VANZANDT and VINCENT, 1983; HOCKING, 1987a and references therein) or even viscosity waves, the latter being capable of existing at very short wavelengths (HOOKE and JONES, 1986).

Having now established that both models have some physical basis, let us concentrate on the simpler models, since these form an excellent basis for later discussion of any of the more complex models.

With regard to model A, it should be noted that θ_s gives a direct measure of the length to depth ratio of the scatterers. The following figure, from HOCKING (1987a), shows this relationship.

What techniques, then can be used to determine the nature of these scatterers?

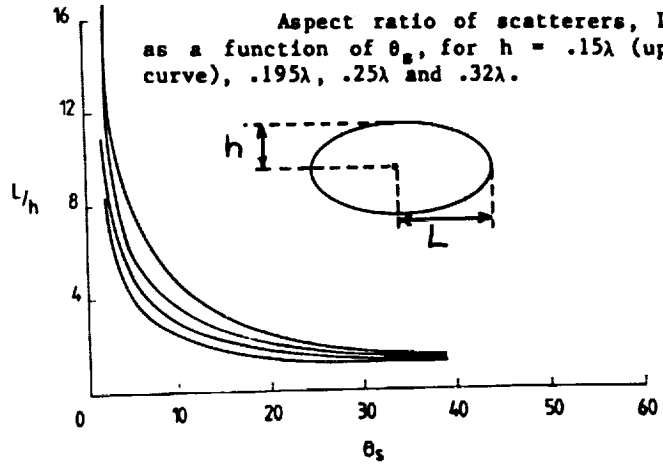

Fig. 13

5.1 Experimental techniques to determine the nature of the scatterers

In the following section a variety of techniques which may be used to determine information about the nature of the scatterers are described and some of the results obtained so far discussed. The list is not, however, exhaustive.

5.1.1 Methods utilizing different beam configurations

One of the simplest methods to investigate the aspect sensitivity of the scatterers is to simply point a narrow beam vertically, and then at several off-vertical angles. The variation in power P as a function of beam tilt angle θ, is then related to θ_s. In fact it can be shown that

$$P(\theta_T) \propto e^{-[\frac{(\theta_{eff}-\theta_T)^2}{\theta_0^2}+\frac{\theta_{eff}^2}{\theta_s^2}]} \tag{65}$$

where θ_{eff} is defined by equation (16), θ_T is the beam tilt direction from the vertical, and the polar diagram of the radar beam is assumed to be of the form $exp\{-(sin^2\theta)/(sin^2\theta_0)\}$ [e.g. appendix A; HOCKING et al (1986); note that the derivation in appendix A corrects an error made in HOCKING et al 1986, in that the important term $\frac{\theta_{eff}^2}{\theta_s^2}$ was neglected in the exponent of e in that paper].

A typical experiment which might be performed is to compare the powers received with a vertical and an off-vertical beam, and use this to deduce θ_s. Utilizing equations (16) and (65) (or equivalently (A4) and (A10)),it is possible to derive the following simple relation between $P(\theta_T)/P(0)$, θ_T and θ_0. If R is defined to be $ln\{P(0)/P(\theta_T\}$ (or $R = 0.23026R_{dB}$, where R_{dB} is the ratio of $P(0)/P(\theta_T)$ expressed in dBs), then

$$\theta_s^2 = \frac{\theta_T^2}{R} - \theta_0^2$$

Typical variations of $P(\theta)$ show an approximately Gaussian fall-off out to about 5°- 10°, and then an approximately constant value beyond this, indicating possibly isotropic turbulence with more anisotropic scatterers either embedded or nearby (e.g. DOVIAK and ZRNIC, 1984). Typical values of θ_s are often in excess of 8°in the troposphere, whilst in the stratosphere at VHF values can be as small as 3°- 4°. The following diagrams from HOCKING et al (1986) summarize some measurements made with the SOUSY radar in Germany (after correction for the error noted above). Note also the tendency for the scatterers to become more isotropic in the high stratosphere.

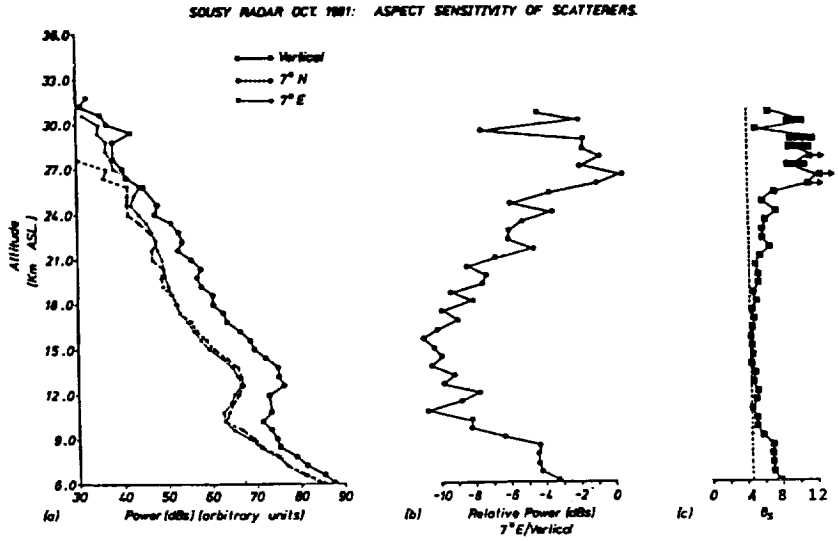

Fig. 4.(a) Plots of 25 h mean powers as a function of altitude for the three beams. Noise has been subtracted. The noise was greatest on the north beam, because of the passage of Cassiopeia A through the beam, and so the signal disappeared into the noise at a lower height than for the other beams. The range effect on the powers has not been removed in this case. (b) Ratio of powers on the 7°E beam and the vertical beam. (c) Assuming that the scatterers had backscatter polar diagrams of the form $\exp(-\sin^2\theta/\sin^2\theta_s)$, this plot gives values of θ_s as a function of height. The vertical broken line shows the minimum θ_s measured. It is clear that above about 18 km, θ_s increased. The widths of each black rectangle gives the error in θ_s associated with a 1 dB increase in $P(7°)/P(0°)$. For θ_s values of greater than about 5°, a 1 dB uncertainty in $P(7°)/P(0°)$ implies a very large uncertainty in θ_s, and these squares with arrows indicate that the possible θ_s value may be as large as 90° for a 1 dB change in $P(7°)/P(0°)$ (i.e. the measurements are very insensitive for $\theta_s \geq 5°$).

Fig. 14

In the mesosphere, θ_s is typically 4°for VHF scatter below 75 km, although on occasions isotropic scatter is also seen. Above 80 km, VHF measurements give θ_s to be about 6°- 8°. At MF, θ_s is typically 2°- 5 °below 80 km, increasing to about 8 - 15°above 80 km (e.g. LINDNER, 1975a,b; VINCENT and BELROSE, 1978. REID (1989) has summarized the various mesospheric measurements.

An alternative means which may be used to determine θ_s is to utilize equation (16). By comparing wind speeds deduced using the DBS method for a beam pointed at say 5°off-zenith to one at say 15°off zenith, it is possible to deduce θ_s from (16), assuming that the value deduced with the 15°beam is the true wind speed. An alternative is to use spaced antenna methods to determine the true wind speed, and then comparisons with the DBS measurements may allow determination of θ_s.

Another interesting determination of θ_s was made by VINCENT and BELROSE (1978),

who compared the powers received on two beams of different polar diagram widths, and used the resultant ratios of powers to determine θ_s. The method yielded results consistent with determinations made by other techniques discussed in this section.

5.1.2 Spatial correlation methods

If one illuminates the sky from a transmitting array which has a very wide polar diagram, and monitors the electric field received at the ground, then the variation of electric field as a function of position is simply the diffraction pattern of the scattering irregularities. The spatial autocorrelation function over the ground can be determined by using an array of dipoles distributed over the ground, recording the signal on each dipole separately and then cross-correlating between dipoles. The spatial autocorrelation function so produced is simply the Fourier transform of the effective polar diagram (ie the combined polar diagrams of the radar beam and the scatterers). If the e^{-1} width of the effective polar diagram is θ_{sb}, then the spatial lag at which the amplitude of the complex autocorrelation function falls to 0.5 is approximately $12.0/\theta_{sb}$ radar wavelengths, where θ_{sb} is expressed in degrees (e.g. HOCKING et al., 1989).

Thus a useful technique for determination of the polar diagram of backscatter is to produce the spatial autocorrelation function in the manner described, and then Fourier transform it. Such a technique has been utilized by LINDNER (1975a, b) in order to study the aspect sensitivity of mesospheric scatterers at an MF frequency of 1.98 MHz. For example, Lindner found typical values for θ_s of about 2°to 5 °below 80 km, and 10°to 15 °above. These results are consistent with later observations using beam-swinging techniques (HOCKING, 1979). The method has not been greatly utilized, however, and deserves further attention.

5.1.3 Spectral methods

It was noted earlier in regard to discussions about extraction of turbulence from spectra that in many cases the main contribution to the spectral width was spectral-broadening due to the finite width of the polar diagram of the radar beam. At the time this was a nuisance, but now it can be turned to good effect. The effective polar diagram is the product between the polar diagram of the radar and the backscatter polar diagram of the scatterers. As seen in appendix A, if θ_{sb} is the e^{-1} half-width of the effective polar diagram (ie the product of the backscatter polar diagram and the radar beam polar diagram) then

$$sin^{-2}\theta_{sb} = sin^{-2}\theta_0 + sin^{-2}\theta_s \tag{66}$$

But from equation (17) the beam-broadening of the spectral width is

$$f_{\frac{1}{2}b} = \frac{2}{\lambda}(1.0) \mid V_{hor} \mid \theta_{\frac{1}{2}}. \tag{67}$$

The total spectral half-power-half-width is given approximately by

$$f_{\frac{1}{2}}^2 = f_{\frac{1}{2}b}^2 + f_{fluct}^2 \tag{68}$$

if we ignore the contribution due to wind-shear. (This last term can in fact reduce $f_{\frac{1}{2}}$, but it is usually fairly small.) Then we can apply our experimentally measured spectral widths to place upper limits on θ_s. That is, if we calculate

$$\theta'_{\frac{1}{2}} = \frac{\lambda}{2} \frac{f_{\frac{1}{2}}}{\mid V_{hor} \mid} \tag{69}$$

then this is a usful upper limit to $\theta_{\frac{1}{2}eff}$, the half-power half-width of the combined polar diagram of the scatterers and the radar beam. In the case that it can be shown that $f_{\frac{1}{2}b} \gg f_{fluct}$, as often happens, then $\theta'_{\frac{1}{2}}$ is a good estimate of $\theta_{\frac{1}{2}eff}$. Then $\theta_{sb} = \theta_{\frac{1}{2}eff}/\sqrt{ln2}$, and equation (66) can be used to deduce θ_s. In the special case that a relatively wide beam is used, so that $\theta_0 \gg \theta s$, $\theta_{sb} = \theta_s$.

The above principles have been used by HOCKING et al.,(1986), and HOCKING (1987a, b) to make estimates of backscatter polar diagram half-widths. The method of using fading times as a crude indicator of "specularity" , as done by for example RASTOGI and ROETTGER (1982) may be also considered as a primitive special case of this method, although that procedure does not really pay proper consideration to the role of the mean wind in determining the fading time through beam-broadening. More recently WOODMAN and CHU (1989) have used similar techniques, but rather than just using the spectral width and assuming Gaussian polar diagrams as done here, they have used the whole spectrum and the one-to one correspondence between the polar diagram of backscatter and the spectrum to determine additional detail about the actual shape of the polar diagram of backscatter and so the irregularities themselves. Woodman and Chu also used a wide beam, but it should be noted that this procedure assumes azimuthal symmetry.

A procedure like this is very useful if there are several types of scatterers in the beam. For example, if scatterers and reflectors described by models A and B both exist in the same radar volume, the spectrum will not be Gaussian, but will comprise two portions; a narrow central component corresponding to the specular reflectors, and a wider component corresponding to the "model A" scatterers. As it turned out, WOODMAN and CHU (1989) saw no evidence of "model B" reflectors, but this is likely to be because their spectra were averaged over 45 min, whilst specular reflectors, if they exist, are likely to be relatively short-lived.

Indeed, evidence for the coexistence of the two types of scatterers coexisting in the same region of space has been given by HOCKING (1987a), and is illustrated in the following diagram. The data are presented because they show yet another useful means of determining information about the scatterers, as well as making the point that both specular reflectors and turbulent scatterers do seem to coexist.

These data were obtained using a hybrid of the beam-swinging and spectral approaches. Two beams were used, one vertical and one off-vertical. A strong signal of very narrow width was seen with the vertical beam, but nothing else, whereas on the off-vertical beam two separate contributions to the spectra were seen; first a broader component corresponding to isotropic bakscatter received through the main lobe of the beam, and secondly the same narrow spectrum as seen with the vertical beam. Clearly the second component was due to leakage from overhead, and comparison of the powers in the specular component observed with the narrow beam and the more isotropic component show that the specular component is some 70 times stronger. The model discussed in Fig. 12 may apply in some cases, but certainly does not here, as it is unlikely that the anisotropic scatterers at the layer edges would be so much stronger than their counterparts in the centre of the layer. Thus this figure does indeed suggest the coexistence of both models, whilst at the same time demonstrating yet another useful technique to determine the aspect-sensitivity and nature of the scatterers.

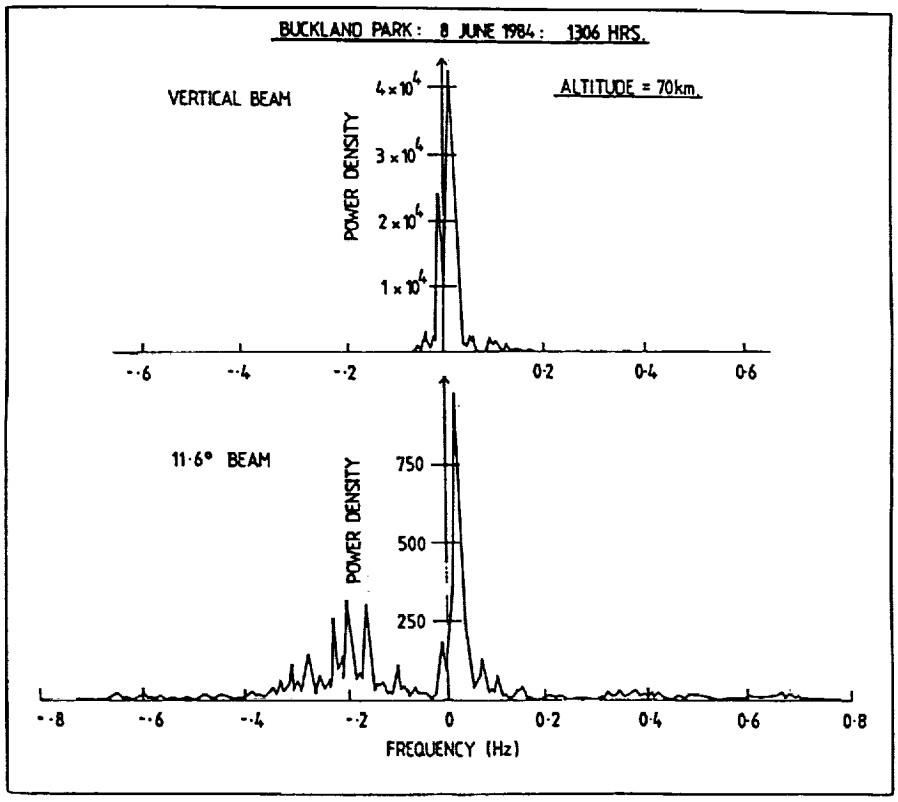

Fig. 15 Spectra recorded with vertical and off-vertical beams of the Buckland Park 2 MHz radar.

5.1.4 Amplitude distributions

The preceding techniques have been designed to make measurements of θ_s, and are particularly powerful if model A is valid. However, there is a useful method which allows the validity of model B to be tested, and which has been used with varying degrees of success in recent years. This is the use of amplitude distributions (e.g. VON BIEL, 1971, 1981; VINCENT and BELROSE, 1978; ROETTGER, 1980a; RAŞTOGI and HOLT, 1981; SHEEN et. al., 1985; HOCKING, 1987b; KUO et al., 1987 amongst others).

There are many variations of this technique, but only the simplest will be discussed here, in order to illustrate the method. If scatter is due to an ensemble of roughly similar scatterers, as might occur in a turbulent patch, then the amplitudes of the resultant distribution will have a so-called "Rayleigh distribution" (RAYLEIGH, 1894). If, however, there is also a much stronger single scatterer in addition to these weaker scatterers, the distribution changes to a so-called "Rice distribution" (RICE, 1944, 1945). The figure below shows how these distributions change as the specular component is made larger. Each curve is parameterized by a parameter called the "Rice parameter", which is a measure of the strength of the specular component divided by the RMS "random" component. For a Rayleigh distribution, this parameter is zero.

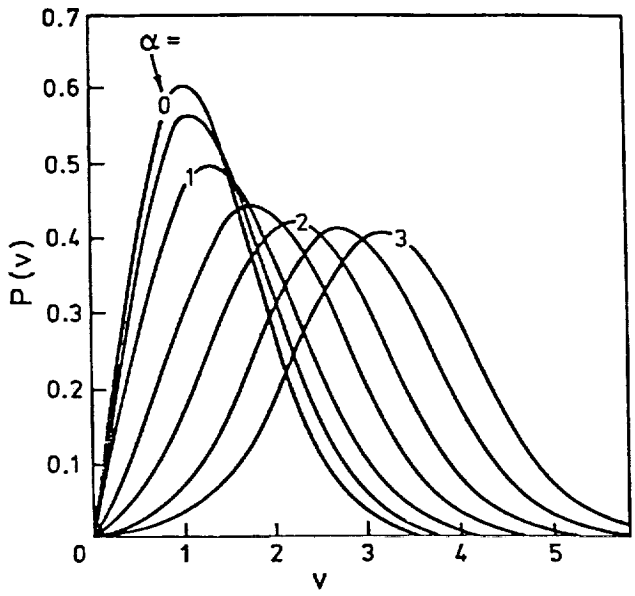

Fig. 16 Rice distributions in steps of $\alpha = 0.5$ as a function of $v = z/\sigma = \sqrt{2} \cdot z/k$, where z = received amplitude, k = RMS scattered power and σ = the standard deviation of each of the inphase and quadrature components of the scattered signal. These plots may also be regarded as the distribution of amplitudes for a constant RMS scatter component $k = \sqrt{2}$ and varying specular component.

Thus in principle, by making histograms of the amplitudes of the received signal and comparing them to the above curves, it is possible to determine if there is a single dominant scatterer within the radar beam. More complex variations on this process exist, including looking at the phase distributions (e.g. ROETTGER, 1980a) and using more complex distributions such as the Nakagami-M distribution (e.g. SHEEN et al., 1985; KUO et al., 1987). The latter generalization is particularly useful if the specular component has undulations on it and causes focussing and de-focussing of the reflected radiation.

Unfortunately, as with almost all techniques, complications exist. For example, if there is more than one specular reflector in the radar volume, then the amplitude distribution changes, and if there are more than about 4, the distribution begins to look almost Rayleigh-like again. Furthermore, if one uses relatively short data sets (less than about 10 mins of data), statistical effects can cause a set of scatterers which should produce a Rayleigh distribution to produce a Rice distribution, which wrongly suggests the existence of a specular component. To properly utilize the so-called Rice parameter one must look at the distributions of the Rice parameter itself; the calculation of several non-zero Rice parameters is not in itself evidence for a non-Rayleigh distribution. The correct interpretation of the Rice parameter is discussed by HOCKING, (1987b).

Nevertheless, the process can be useful, as illustrated by the many authors listed previously. An interesting example is shown in fig.17 below, which was taken from HOCKING (1987b).

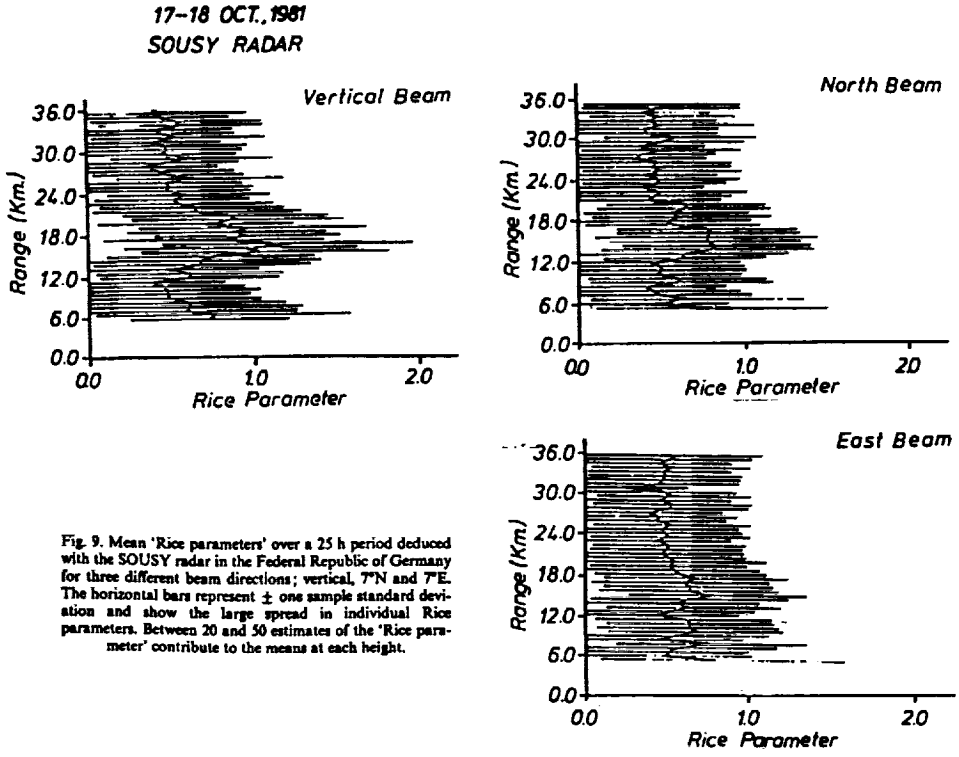

Fig. 9. Mean 'Rice parameters' over a 25 h period deduced with the SOUSY radar in the Federal Republic of Germany for three different beam directions; vertical, 7°N and 7°E. The horizontal bars represent ± one sample standard deviation and show the large spread in individual Rice parameters. Between 20 and 50 estimates of the 'Rice parameter' contribute to the means at each height.

Fig. 17

This diagram shows the height profile of the mean Rice parameter ($< \alpha >$) as a function of height measured with the SOUSY radar, using a vertical beam and two off-vertical beams, one directed at 7°off-vertical to the North, and one at 7°off-vertical to the East. Note the increase in $< \alpha >$ just above the tropopause, when observing with the vertical beam, indicating the presence of a few dominant reflectors within the radar volume in the stratosphere. Notice also that there is still a non-Rayleigh character to the scattering process on the North beam, but on the East beam the mean Rice parameter is fairly constant with height and consistent with a Rayleigh process.

One possible interpretation of these results is that the scatterers are elongated in the Eastward direction compared to the Northward (ie aligned along the mean wind vector, which was predominately Eastward at the time). If such an elongation existed, then the polar diagram of backscatter would be narrower in the East-West direction, and so the half-power half-width may be substantially less than 7°and not show an effect on the 7°off-vertical beam; only the effects of the turbulent scatter are seen. In the North-South direction, the polar diagram would be wider, and some contribution from these scatterers may still show.

Alternatively, one might invoke model B, and speculate that flat specular reflectors exist with small wrinkles, but that there were a wider range of Fourier components in the North-South direction, causing a broadened polar diagram in this direction.

It is clear from the above techniques that there are a multitude of techniques available to enable the nature of the scatterers to be understood. However, there are still many unresolved

issues about these scatterers, and the application of the above procedures is to be actively encouraged, in the hope of eventually fully understanding the scattering and reflecting processes, and the parameters which describe them. The importance of knowing these characteristics has already been stressed.

6 Less easily determined target parameters

The discussion so far has concentrated on parameters which can be inferred fairly directly from the radar measurements. There are, however, other parameters which can be deduced with a little extra work. For example, VINCENT and REID (1983) showed how, by using two off-vertical beams, measurements of the gravity-wave and turbulent momentum fluxes could be calculated. The momentum flux is not actually a target parameter, and so has not been discussed here greatly, but it nevertheless is a parameter which affects the targets, and knowledge about is most desirable. Another example is the Brunt-Vaisala frequency. Normally this is very difficult to measure, but if the mean winds are light, then spectral analysis of the time series of velocity measurements can be used to measure the Brunt-Vaisala frequency. That is, the spectrum shows a cutoff at the Brunt-Vaisala frequency, and this in turn allows determination of the temperature gradient (e.g. ROETTGER, 1980b).

DEWAN (1981) and WOODMAN and RASTOGI (1984) have shown how careful measurements of the temporal and spatial distribution of the occurrence of thin turbulent layers can be used to infer the mean turbulent diffusion coefficient in the stratosphere, as distinct from the diffusion coefficient within a turbulent layer (the latter can be determined from equation (38)).

High resolution studies can also be used to infer something about the nature of the scatterers; for example ROETTGER and SCHMIDT (1979) used a resolution of 30m to observe cat's-eye structures in the stratosphere, confirming that at least some of the observed turbulent layers are due to dynamical instability. REID et al. (1987) have observed similar features in the mesosphere. Other studies which allow information about the nature of the scatterers to be obtained include, for example, those by KLOSTERMEYER and RUESTER (1980, 1981), and YAMAMOTO et al. (1987, 1988); in these studies relations between power bursts and buoyancy-wave oscillations were investigated.

By using radars in conjunction with other instruments, further information can be deduced. A good example is the use of acoustic waves to act as reflectors for VHF radar waves, as done with the RASS system at the MU radar in Japan. With this instrument, it is possible to measure temperature profiles in the atmosphere. The use of such hybrid systems in the future is likely to be of great benefit.

Of course, by using long time series of velocities, one can determine other characteristics of the scattering region, like the buoyancy wave spectra, tidal amplitudes, planetary wave amplitudes, and a whole host of dynamical quantities. In a broad sense one might like to think of these as "target parameters" of a sort, but these are beyond the scope of the current paper.

7 Conclusions

The main parameters which can be deduced directly from radar observations of the atmosphere have been discussed. It is clear that it is not possible to make best use of the observations without better understanding the scattering process, and the ways in which the scatterers are

formed. Methods for deducing more information about the scatterers have been described, as well as some procedures by which routine information like wind speeds, turbulence intensities, and scatterer shapes, can be deduced. The need for more observations of this sort is pressing.

Appendix A: Effective pointing angle and beamwidth for anisotropic scatter

As pointed out by ROETTGER (1981), an anisotropy in the scattering mechanism alters the effective pointing angles for an off-vertical radar. Such anisotropy also alters the effective beamwidth and this is important for the work in this paper. Let the polar diagram of backscatter for the scatterers be

$$P_s(\theta) \propto e^{-\frac{sin^2\theta}{sin^2\theta_s}}$$

and the two way polar diagram for a vertically pointing radar be (A1)

$$P_R(\theta) \propto e^{-\frac{sin^2\theta}{sin^2\theta_0}} \quad \text{(A2)}$$

Then for a radar pointed off-vertical by angle θ_T in the azimuth direction $\phi = 0$, the polar diagram at angle (θ, ϕ) is

$$P_{RT}(\theta,\phi) \propto e^{\left\{-\left[\frac{(sin\theta sin\phi)^2+(sin\theta cos\phi - sin\theta_T)^2}{sin^2\theta_0}\right]\right\}}. \quad \text{(A3)}$$

(Note that the expression $exp[-sin^2(\theta - \theta_T)/sin^2\theta_0)$ (which has in the past been used to represent a tilted beam) is NOT a good approximation, as that describes an annulus around the zenithal point at a mean angle θ_T.) When the effects of the polar diagram of the scatterers are included, the effective polar diagram is the product of (A1) and (A3). This is a maximum when the derivative of the exponent with respect to $sin\theta$ is zero, or at

$$sin\theta_{eff} = sin\theta_T \left[1 + \frac{sin^2\theta_0}{sin^2\theta_s}\right]^{-1} \quad \text{(A4)}$$

For θ_0, θ_s less than about 10°, this approximates to

$$sin\theta_{eff} = sin\theta_T \left[1 + \frac{\theta_0^2}{\theta_s^2}\right]^{-1}$$

Thus the effective pointing angle is given by (A4), and horizontal wind speeds will be underestimated by the factor

$$R_1 = \left[1 + \frac{\theta_0^2}{\theta_s^2}\right]. \quad \text{(A5)}$$

if one uses say equation (12) without any correction. This is in fact only approximate - to properly determine the actual measured radial velocity, equation (35) of HOCKING (1983a) should be integrated (including an aspect sensitivity for the scatterers) to produce the expected power spectrum; this will not have a maximum at the exact point described by (A4), but it will be close.

The half-width of the effective beam can be found by finding the angles (θ, ϕ) where the effective polar diagram [i.e. the product of (A1) and (A3)] falls to one half of the value at $(\theta, \phi) = (\theta_{eff}, 0)$. Consider only the line $\phi = 0$. Then the product of (A1)and (A3) gives

$$e^{\left\{-\left[\frac{(sin\theta - sin\theta_T)^2}{sin^2\theta_0} + \frac{sin^2\theta}{sin^2\theta_s}\right]\right\}} \quad \text{(A6)}$$

and we seek the two angles $(\theta_{\frac{1}{2}})_{1,2}$ where this falls to one half of the value at $\theta = \theta_{eff}$. Some algebraic manipulation soon shows that a quadratic in $sin\theta$ results, which has two roots at

$$(\theta_{\frac{1}{2}})_{1,2} = sin\theta_{eff} \pm \sqrt{ln2}.sin\theta_0 \left[1 + \frac{\theta_0^2}{\theta_s^2}\right]^{-\frac{1}{2}} \tag{A7}$$

(for θ_0, θ_s less than about 10°), and this shows that the effective half-power half-width is

$$R_2 = \left[1 + \frac{\theta_0^2}{\theta_s^2}\right]^{-\frac{1}{2}} \tag{A8}$$

times the half-width of the radar alone. Notice that this ratio is independent of the radar tilt direction, at least out to angles of 10-15°.

Equivalently, we can write that the effective half-power half-width $\theta_{eff\frac{1}{2}}$ obeys the relation

$$sin^{-2}(\theta_{eff\frac{1}{2}}) = sin^{-2}(\theta_{\frac{1}{2}}) + sin^{-2}(\theta_{s\frac{1}{2}}), \tag{A9}$$

where $\theta_{\frac{1}{2}}$ is the half power half width of the radar beam and $\theta_{s\frac{1}{2}}$ is the half-power half-width of the backscatter polar diagram of the scatterers.

Now let use address the issue of how the power received by the radar changes as a function of tilt angle θ_T. The power received by the vertical beam can be found by integrating over the beam, and for a Gaussian polar diagram this integral is proportional to $(\theta_{eff\frac{1}{2}})^2$ where $\theta_{eff\frac{1}{2}}$ is the effective half-power half-width of the combined polar diagrams of the radar and the scatterers. When the radar beam is phased to look at an off-vertical angle θ_T, the peak power will be reduced by a factor

$$f1 = e^{\{-\frac{(\theta_{eff}-\theta_T)^2}{\theta_0^2}\}}$$

because the peak returned power is returned from θ_{eff} and not θ_T, and then by a further factor

$$f2 = e^{\{-\frac{\theta_{eff}^2}{\theta_s^2}\}}$$

bacause of the reduction in power due to the polar diagram of backscatter of the scatterers.

Thus the total received power will be proportional to the product of $f1$ and $f2$, and then multiplied by the effective beam half-power half-width squared. Thus the received power on the off-vertical beam divided by that received on the vertical beam is equal to

$$\frac{f1.f2.(\theta_{eff\frac{1}{2}})^2}{(\theta_{eff\frac{1}{2}})^2}$$

or

$$\frac{P(\theta_T)}{P(0)} = exp\left\{-\left[\frac{(\theta_{eff} - \theta_T)^2}{\theta_0^2} + \frac{\theta_{eff}^2}{\theta_s^2}\right]\right\} \tag{A10}$$

Note that this final expression corrects an error in the original derivation of HOCKING et al, (1986), in which the factor $f2$ was neglected.

References

Adams, G.W., D.P. Edwards and J.W. Brosnahn, The imaging Doppler interferometer; Data analysis, *Rad. Sci., 20*, 1481-1492, 1985.

Atlas, D., *Advances in Geophysics*, vol 10, 317 pp,Academic New York, 1964.

Atlas, D., R.C. Srevastava and P.W. Sloss, Wind shear and reflectivity Gradient effects on Doppler radar spectra, II, *J.Appl.Meteor.,8*, 384-388, 1969.

Austin, G.L., R.G.T. Bennett,and M.R. Thorpe, The phase of waves partially reflected from the lower ionosphere, *J.Atmos.Terr.Phys., 31*, 1099-1106, 1969.

Barat, J., Some characteristics of clear air turbulence in the middle stratosphere, *J.Atmos.Sci., 39*, 2553-2564, 1982.

Batchelor, G.K., *The theory of homogeneous turbulence*, Cambridge University Press, New York, 1953.

Bohne, A.R., Radar detection of turbulence in precipitation environments,*J.Atmos.Sci., 39*, 1819-1837., 1982.

Bolgiano, R., Jr., *The general theory of turbulence - turbulence in the atmosphere, in "Winds and turbulence in the stratosphere, mesopshere and ionosphere"*, ed K. Rawer, p371, North-holland, Amsterdam, 1968.

Bracewell, R.N., *The Fourier Transform and Its Applications*, 444pp.,McGraw-Hill, New York, 1978.

Briggs, B.H., Radar observations of atmospheric winds and turbulence: a comparison of techniques, *J.Atmos.Terr.Phys., 42*, 823-833, 1980.

Briggs, B.H., The analysis of spaced sensor records by correlation techniques, *Handbook for MAP, vol.13*, Ground based techniques, 166-186, Univ. of Illinois, Urbana, 1984.

Briggs, B.H. and R.A.Vincent, Some theoretical considerations on remote probing of weakly scattering irregularities, *Aust.J.Phys., 26*, 805-814, 1973.

Budden, K.G., Effect of electron collisions on the formulas of magnetoionic theory, *Radio Sci., 69D*, 191-211, 1965.

Caughey S.J. ,B.A. Crease, D.N. Asimakapoulos, and R.S. Cole, Quantitative bistatic acoustic sounding of the atmospheric boundary layer, *Q. J. R. Meteorol. Soc, 104*, 147-161, 1980.

Crane, R.K., A review of radar observations of turbulence in the lower stratosphere, *Radio Sci., 15.* 177-194, 1980.

Croft, T.A., Sky-wave backscatter: a means of observing our environment at great distances. *Revs. Geophys. Space Phys., 10* , 73-155, 1972.

Dewan, E.M., Turbulent vertical transport due to thin intermittent mixing layers in the stratosphere and other stable fluids, *Science, 211*, 1041-1042, 1981.

Doviak, R.J., and D.S. Zrnic, Reflection and scatter formula for anisotropically turbulent air, *Radio Sci., 19*, 325-336, 1984.

Farley, D.T., H.M. Ierkic, and B.G. Fejer, Radar interferometry : a new technique for studying plasma turbulence in the ionosphere, *J.Geophys.Res., 86*, 1467-1472, 1981.

Fukao, S., K.Wakasugi, and S.Kato, Radar measurement of short-period atmospheric waves and related scattering properties at the altitude of 13-25 km over Jicamarca, *Radio Sci., 15*, 431-438, 1980a.

Fukao, S., T.Sato, R.M. Harper,and S. Kato, Radio wave scattering from the tropical mesosphere observed with the Jicamarca radar,*Radio Sci., 15*, 447-457, 1980b.

Fukao, S., T. Sato, P.T. May, T. Tsuda, S. Kato, M. Inaba, and I. Kimura, A systematic error in MST/ST radar wind measurement induced by a finite range volume effect,1, Observational results, *Radio Sci., 23*, 59-73, 1988a.

Fukao, S., M. Inaba, I. Kimura, P.T. May, T. Sato, T. Tsuda, and S. Kato, A systemic error in MST/ST radar wind measurement induced by a finite range volume effect,2, Numerical considerations, *Radio Sci.,23*, 74-82, 1988b.

Gage, K.S., and Balsley, B.B., Doppler radar prob-ing of the clear atmosphere,*Bull. Am. Meteorol. Soc., 59*, 1074-1093, 1978.

Gage,K.S., and J.L.Green, Evidence for specular reflection from monostatic VHF radar observations of the stratosphere, *Radio Sci., 13*, 991-1001, 1978.

Gage, K.S., J.L.Green, and T.E.VanZandt, Use of Doppler radar for the measurement of atmospheric turbulence parameters from the intensity of clear air echoes, *Radio Sci., 15*, 407-416, 1980.

Gage,K.S., B.B. Balsley, and J.L. Green, Fresnel scattering model for the specular echoes observed by VHF radars, *Radio Sci., 16*, 1447-1453, 1981a.

Gage, K.S., W.L. Ecklund, and B.B. Balsley, A modified Fresnel scattering model for the parameterization of Fresnal returns, *Radio Sci., 20*, 1493-1502, 1985.

Green, J.L., and K.S.Gage, Observations of stable layers in the troposphere and stratosphere using VHF radar, *Radio Sci., 15*, 395-405, 1980.

Green, J.L. and K.S. Gage, A Re-examination of the range resolution dependence of backscattered power observed by VHF radars at vertical incidence, *Radio Sci., 20*, 1001-1005, 1985.

Gregory, J.B., and R.A. Vincent, Structure of pertially reflecting regions in the lower ionosphere, *J. Geophys. Res., 75*, 6387-6389, 1970.

Hitschfeld, W., and A.S.Dennis, *Measurement and calculation of fluctuations in radar echoes from snow* , Sci. Rep. MW-23, McGill Univ., Montreal, Canada, 1956.

Hocking, W.K., Angular and temporal characteristics of partial reflections from the D-region of the ionosphere, *J.Geophys. Res., 84*, 845-851, 1979.

Hocking,W.K., and R.A. Vincent, Comparative observations of D region HF partial reflections at 2 and 6 MHz, *J.Geophys. Res., 87*, 7615-7624, 1982a.

Hocking, W.K. and R.A. Vincent, A comparison between HF partial reflection profiles from the D-region and simultaneous Langmuir probe electron density neasurements,*J. Atmos. Terr. Phys., 44*, 843-854, 1982b.

Hocking W.K., On the extraction of atmospheric turbulence parameters from radar backscatter Doppler spectra I, Theory, it J. Atmos. Terr. Phys., 45, 89-102, 1983a.

Hocking, W.K., Mesospheric turbulence intensities measured with a HF radar at 35°S, II, *J.Atmos. Terr.Phys., 45*, 103-114, 1983b.

Hocking, W.K. The spaced antenna drift method, *Handbook for MAP, vol.9*, 171-186, Univ. of Illinois, Urbana, 1983c.

Hocking, W.K., and J. Roettger, Pulse-length dependence of radar signal strengths for Fresnel backscatter,*Radio Sci., 18*, 1312-1324, 1983.

Hocking, W.K., G. Schmidt, and P. Czechowsky, *Absolute calibration of the SOUSY VHF stationary radar*, Max-Planck-Instut fur Aeronomie report MPAE-W-00-83-14, Katlenburg-Lindau, F.R.G., 1983

Hocking, W.K., R. Ruester and P. Czechowsky, *Observation and measurement of turbulence and stability in the middle atmosphere with a VHF radar*, University of Adelaide internal report ADP-335, University of Adelaide, Adelaide, S.A. Australia, 1984

Hocking, W.K., Measurement of turbulent energy dissipation rates in the middle atmosphere by radar techniques: a review, *Radio Sci., 20*, 1403-1422, 1985.

Hocking W.K., R. Ruester and P. Czechowsky, Absolute reflectivities and aspect sensitivities of VHF radio wave scatterers measured with the SOUSY radar, *J.Atmos.Terr.Phys., 48*, 131-144, 1986.

Hocking, W.K., Observation and measurement of turbulence in the middle atmosphere with a VHF radar,*J.Atmos. Terr. Phys., 48*, 655-670, 1986.

Hocking, W.K., Radar studies of small scale structure in the upper middle atmosphere and lower ionosphere, *Adv. Space Res., 7*, 327-338, 1987a

Hocking, W.K., Reduction of the effects of non-stationarity in studies of amplitude statistics of radio wave backscatter, *J. Atmos. terr. Phys., 49*, 1119-1131, 1987b

Hocking, W.K., Two years of continuous measurements of turbulence parameters in the upper mesosphere and lower thermosphere made with a 2-MHz radar,*J. Geophys. Res., 93*, 2475-2491, 1988

Hocking, W.K., May, P.T., and Roettger, J., Interpretation, reliability and accuracies of parameters deduced by the spaced antenna method in middle atmosphere applications, *Pure and Appl. Geophys.*, 1989, in press.

Hooke, W.H., and R.M. Jones, Dissipative waves excited by gravity-wave encounters with the stably stratified Planetary Boundary Layer, *J. Atmos. Sci., 43*, 2048-2060, 1986.

Klaassen, G.P., and W.R. Peltier, Evolution of finite amplitude Kelvin-Helmholtz billows in two spatial dimensions, *J. Atmos. Sci., 42*, 1321-1339, 1985.

Klostermeyer, J. and R. Ruester, Radar observation and model computation of a jet stream-generated Kelvin-Helmholtz instability, *J. Geophys. Res., 85*, 2841-2846, 1980.

Klostermeyer, J. and R. Ruester, Further study of a jet stream-generated Kelvin-Helmholtz instability,*J. Geophys. Res., 86*, 6631-6637, 1981.

Kuo, F.-S.,C.-C. Chen, S.I. Liu, J. Roettger, and C.H. Liu, Systematic behaviour of signal statistics of MST radar echoes from clear air and their interpretation, *Radio Sci., 22*, 1043-1052, 1987.

Labitt, M., *Some basic relations concerning the radar measurement of air turbulence*, Mass. Inst. of Technol., Lincoln Lab., Work. Pap. 46WP-5001, 1979.

Lilly, D.K., D.E. Waco and S.I. Adelfang, Stratospheric mixing estimated from high-altitude turbulence measurements,*J. Appl. Meteorol., 13*, 488 - 493, 1974.

Lindner, B.C., The nature of D-region scattering of vertical incidence radio waves, I. Generalized statistical theory of diversity effects between spaced receiving antennas, *Aust.J.Phys., 28*, 163-170, 1975a.

Lindner, B.C., The nature of D-region scattering of vertical incidence radio waves, II., Experimental observation using spaced antenna reception, *Aust.J.Phys., 28*, 171-184, 1975b.

Manson, A.H., M.W.J. Merry, and R.A. Vincent, Relationship between the partial reflection of radio waves from the lower ionosphere and irregularities as measured by rocket probes, *Radio Sci., 4*, 955-958, 1969.

Mathews J.D., J.H. Shapiro and B.S. Tanenbaum, Evidence for distributed scattering in D-region partial-reflection processes, *J.Geophys. Res. 78*, 8266. 1973.

Mathews, J.D., J.K. Breakall, and M.P. Sulzer, The moon as a calibration target of convenience for VHF-UHF radar systems, *Radio Sci., 23*, 1-12, 1988.

May, P.T., S. Fukao, T. Tsuda, T. Sato and S. Kato, The effect of thin scattering layers on the determination of wind by Doppler radars, *Radio Sci., 23*, 83-94, 1988.

Ottersten, H., Radar backscattering from the turbulent clear atmosphere, *Radio Sci., 12*, 1251-1255, 1969.

Peltier, W.R., J.Halle, and T.L.Clark, The evolution of finite-amplitude Kelvin-Helmholtz Billows, *Geophys. Astrophys. Fluid Dyn., 10*, 53-87, 1978.

Pfister, W., The wave-like nature of inhomogeneities in the E-region, *J.Atmos.Terr.Phys., 33*, 999-1025, 1971.

Rastogi P.K. and O. Holt, On detecting reflections in presence of scattering from amplitude statistics with application to D-region partial reflections,*Radio Sci. 16*, 1431-1443, 1981.

Rastogi, P.K. and J. Roettger, VHF radar observations of coherent reflections in the vicinity of the tropopause,*J. Atmos. Terr. Phys., 44*, 461-469, 1982.

Ratcliffe, J.A., Some aspects of diffraction theory and their application in the ionosphere, *Rep. Prog. Phys., 19*, 188-267, 1956.

Rayleigh, Lord(J.W.Strutt),*Theory of Sound*, vol.1, pp.35-42. Macmillan, New York, 1894.

Reid, I.M., R. Ruester and G. Schmidt,*Nature*, 327, 43, 1987.

Reid, I.M., Radar observations of stratified layers in the mesosphere and lower thermosphere (50-100 km), *Adv. Space Res.*, 1989 (in press).

Rice,S.O., Mathematical analysis of random noise, *Bell Syst, Tech.J., 23*, 282-332, 1944.

Rice,S.O., Mathematical analysis of random noise, *Bell Syst. Tech.J.,24*, 46-156, 1945.

Roettger, J., Reflection and scattering of VHF radar signals from atmospheric refractivity structures, *Radio Sci., 15*, 259-276, 1980a.

Roettger, J., Structure and dynamics of the stratosphere and mesosphere revealed by VHF radar investigations, *Pure Appl. Geophys., 118*, 494-527, 1980b.

Roettger, J., Investigations of lower and middle atmosphere dynamics with spaced antenna drifts radars, *J.Atmos.Terr.Phys., 43*, 277-292, 1981.

Roettger, J., and C.H.Liu, Partial reflection and scattering of VHF radar signals from the clear atmosphere, *Geophys. Res. Lett., 5*, 357-360, 1978.

Roettger, J. and G. Schmidt, High-resolution VHF radar soundings of the troposphere and stratosphere, *IEEE Trans. Geosci. Electron., GE-17*, 182-189, 1979

Roettger, J. and H.M. Ierkic, Postset beam steering and interferometer applications of VHF radars to study winds, waves and turbulence in the lower and middle atmosphere, *Radio Sci., 20*, 1461-1480,1985.

Sato,T., and R.F.Woodman, Fine altitude resolution observations of stratospheric turbulent layers by the Arecibo 430 MHz radar, *J.Atmos. Sci., 39*, 2553-21564, 1982.

Sheen D.R., C.H. Liu and J. Roettger, A study of signal statistics of VHF radar echoes from clear air,*J. Atmos. Terr. Phys., 47*, 675-684, 1985.

Sloss,P.W.,and D.Atlas, Wind shear and reflectivity gradient effects on Doppler radar spectra, *J.Atmos.Sci., 25*, 1080-1089, 1968.

Tatarski, V.I.,*Wave propagation in a turbulent medium*, McGraw-Hill, New York, 1961.

Tatarski, V.I., *The effects of the turbulent atmosphere on wave propagation*, Keter Press, Jerusalem, 1971.

Thrane, E. V., and B. Grandal, Observations of finescale structure in the mesosphere and lower thermosphere, *J. Atmos. Terr. Phys., 43*, 179-189, 1981.

VanZandt,T.E., J.L.Green, K.S.Gage, and W.L.Clark, Vertical profiles of refractivity turbulence structure constant: Comparison of observations by the Sunset radar with a new theoretical model,*Radio Sci., 13*, 819-829, 1978.

VanZandt,T.E., K.S.Gage and J.M.Warnock, An improved model for the calculation of profiles of and in the free atmosphere from background profiles of wind, Temperature and humidity, paper presented at *20th Conference on Radar Meteorology, Am.Met.Soc.*, Boston, Mass., Nov.30-Dec.3,1981.

Van Zandt, T.E., and R.A. Vincent, Is VHF Fresnel reflectivity due to low frequency buoyancy waves?, *Handbook for MAP, vol. 9*, p 78-80, Univ. of Illinois, Urbana, 1983.

Vincent, R.A., The interpretation of some observations of radio waves scattered from the lower ionosphere, *Aust.J.Phys., 26*, 815-827, 1973.

Vincent, R.A. and J.S. Belrose, The angular distribution of radio waves partially reflected from the lower ionosphere,*J. Atmos. Terr. Phys., 40*, 35-47, 1978

Vincent, R.A., and I.M. Reid, HF Doppler measurements of mesospheric gravity wave momentum fluxes, *J. Atmos. Sci., 40*, 1321-1333, 1983.

Vincent, R.A., B. Candy and B.H. Briggs, Measurements of antenna polar diagrams and efficiencies using a phase-switched interferometer, *Handbook for MAP, vol. 20*, p409-409, Univ. of Illinois, Urbana, 1986

Von Biel, H.A., Amplitude distributions of D-region partial reflections, *J. Geophys. Res, 76*, 8365-8367, 1971.

Von Biel, H.A., A statistical assessment of synoptic D-region partial reflection data,*J. Atmos. Terr. Phys., 43*, 225-230, 1981

Waterman, A.T., Techniques for measurement of vertical and horizontal velocities; monstatic vs. bistatic measurements, *Handbook for MAP, vol 9*, 164-169, Univ. of Urbana, 1983.

Waterman, A.T., T.Z. Hu, P. Czechowsky and J. Roettger, Measurement of anisotropic permittivity structure of upper troposphere with clear-air radar, *Radio Sci., 20*, 1580-1592, 1985

Weinstock, J., On the theory of turbulence in the buoyancy subrange of stably stratified flows, *J.Atmos.Sci., 35*, 634-649, 1978a.

Weinstock,J., Vertical turbulent diffusion in a stably stratified fluid, *J.Atmos.Sci., 35*, 1022-1027, 1978b.

Weinstock,J., Using radar to estimate dissipation rates in thin layers of turbulence, *Radio Sci., 16*, 1401-1406, 1981.

Woodman, R.F.and A.Guillen, Radar observations of winds and turbulence in the stratosphere and mesosphere, *J.Atmos. Sci., 31*, 493-505, 1974

Woodman, R.F. and P.K.Rastogi, Evaluation of effective eddy diffusive coefficients using radar observations of turbulence in the , stratosphere, *Geophys. Res. Letts., 11*, 243-246, 1984.

Woodman,R.F., Spectral moment estimation in MST radars, *Radio Sci., 20*, 1185-1195, 1985.

Woodman, R.F. and Y-H Chu, Aspect sensitivity measurements of VHF backscatter made with the Chung-Li radar: plausible mechanisms, *Radio Sci.*, 1989 (accepted)

Yamamoto, M., T. Tsuda, S. Kato, T. Sato, and S. Fukao, A saturated inertia gravity wave in the mesosphere observed by the middle and upper atmosphere radar, *J. Geophys. Res., 92*, 11993-11999, 1987.

Yamamoto, M., T. Tsuda, S. Kato, T. Sato, and S. Fukao, Interpretation of the structure of mesospheric turbulence layers in terms of inertia gravity waves, *Physica Scripta, 37*, 645-650, 1988.

Zrnic,D.S., Estimation of spectral moments for weather echoes, *IEEE Trans. Geosci. Electron., GE-17*, 113-128, 1979.